



EVSE Characterization

A Next-Gen Profiles Project Report

December 2023

Disclaimer

This work was prepared as an account of work sponsored by an agency of the United States government. Neither the United States government nor any agency thereof, nor any of their employees, nor any of their contractors, subcontractors or their employees, makes any warranty, express or implied, or assumes any legal liability or responsibility for the accuracy, completeness, or any third party's use or the results of such use of any information, apparatus, product, or process disclosed, or represents that its use would not infringe privately owned rights. Reference herein to any specific commercial product, process, or service by trade name, trademark, manufacturer, or otherwise, does not necessarily constitute or imply its endorsement, recommendation, or favoring by the United States government or any agency thereof or its contractors or subcontractors. The views and opinions of authors expressed herein do not necessarily state or reflect those of the United States government or any agency thereof, its contractors or subcontractors.

Authors

Richard “Barney” Carlson, Idaho National Laboratory (INL)

Omer Onar, Oak Ridge National Laboratory (ORNL)

Acknowledgments

The authors would like to acknowledge the valuable guidance and input provided during this report. The authors are grateful for the contributors in the following list. Their feedback, guidance, and review proved invaluable.

Contributors:

Lee Slezak, Department of Energy, Vehicle Technologies Office

Daniel Dobrzynski, Argonne National Laboratory (ANL)

Landon Wells, Argonne National Laboratory (ANL)

Sam Thurston, Argonne National Laboratory (ANL)

Benny Varghese, Idaho National Laboratory (INL)

Richard “Barney” Carlson, Idaho National Laboratory (INL)

Andrew Meintz, National Renewable Energy Laboratory (NREL)

Ed Watt, National Renewable Energy Laboratory (NREL)

Keith Davidson, National Renewable Energy Laboratory (NREL)

Namrata Kogalur, National Renewable Energy Laboratory (NREL)

Omer Onar, Oak Ridge National Laboratory (ORNL)

This report INL/RPT-24-76181 was prepared by Idaho National Laboratory for the U.S. Department of Energy, Office of Energy Efficiency and Renewable Energy, Vehicle Technologies Office.

List of Acronyms

AC	Alternating Current
CCS	Combined Charging System
CCS-1	Combined Charging System (-1 is the North American version)
CHAdeMO	CHArge de Move
DC	Direct Current
DOE	U.S. Department of Energy
EV	Electric Vehicle
EVSE	Electric Vehicle Supply Equipment
INL	Idaho National Laboratory
kW	Kilowatt
OCPP	Open Charge Point Protocol
ORNL	Oak Ridge National Laboratory
SCM	Smart Charge Management
THD	Total Harmonic Distortion
V	Volts
WPT	Wireless Power Transfer
XFC	Extreme Fast Charger

Executive Summary

As part of the U.S. DOE EVs@Scale consortium Next-Generation Profiles project, results and analysis from the characterization of high-power conductive and wireless charging infrastructure are presented. This characterization was conducted over a wide range of DC output current and DC voltage charging for nominal test conditions and off-nominal test conditions. Test plans and procedures were developed to define the test configurations and requirements, measurement parameters, and test procedures used throughout testing.

Results from a 2023 study conducted on electric vehicle supply equipment (EVSE) characterization by Idaho National Laboratory (INL) and Oak Ridge National Laboratory (ORNL) include one 350 kW capable EVSE using a liquid-cooled combined charging system-1 (CCS-1, North American version) cable and connector and an ORNL-developed 100-kW polyphase wireless charger.

Characterization results during nominal operation show the AC-to-DC power transfer efficiency for the 350kW conductive EVSE is 95.1% peak and is >92% when the AC power is at least 50 kW. The power quality of the 350 kW conductive EVSE is also measured during nominal conditions. The power factor is >0.91 for power transfer above 50 kW AC input during nominal conditions with a maximum power factor of 0.975. The AC current harmonics produced by the EVSE as measured at the AC input connection to the EVSE is <25% harmonics for power transfer greater than 50 kW and <10% harmonics for power transfer greater than 180 kW.

EVSE characterization is conducted during AC grid input off-nominal conditions involving AC voltage deviation (426 VAC to 518 VAC), frequency deviation (58.8–61.2 Hz), and 5% harmonics injection. The 350-kW-capable EVSE power transfer is not notably impacted by the voltage deviation and frequency deviation, as indicated by very low DC current ripple during the off-nominal test conditions. However, during the 5% harmonics injection during the 350-kW power transfer test condition, the DC current ripple exceeded 14%, and the phase-to-phase AC current unbalance exceeded 18.9%. For the off-nominal AC grid input test cases, the EVSE power transfer continues as requested, except when AC input voltage drops below 418 VAC (13% voltage sag), resulting in the interruption of the EVSE power transfer until the AC input voltage recovers to greater than 418 AC.

Characterization of the 350-kW conductive EVSE at nominal conditions is performed for a high-utilization scenario that involves three consecutive, full-power, 10-minute charge sessions separated by a 5-minute rest period between the charge sessions. This scenario represents three EVs charging at one EVSE, each for 10 minutes. The 5-minute rest period represents the time for the one EV to end its charge session, be unplugged, driven away, and for a second EV to arrive, be plugged in, and begin a charge session. The high-utilization characterization of the 350 kW EVSE results in a full-power transfer (346kW DC) for the first 6 minutes of the charge session for

the first EV and is followed by 90 AMP DC charging thereafter. This 90 AMP DC limited-charge rate is due to an exceeded thermal threshold associated with the liquid-cooled cable thermal management system. The 90 AMP DC limit persists throughout all subsequent charge sessions until the thermal management system is reset, as accomplished by cycling 480 VAC input power to the EVSE. This characterization result indicates the thermal management system is insufficient for consecutive full-power charge sessions.

Smart charge management curtailment response latency and ramp rates characterization are conducted for the 350 kW EVSE at four initial power transfer conditions. Three types of curtailment requests are conducted, each at 65 AMP and 54 kW. The three curtailment request types are *ChargePointMaxProfile*, *TxDefaultProfile*, and *TxProfile*. The latency of the EVSE power transfer to respond to the curtailment request is roughly 3 seconds on average, but it varies greatly, ranging from 0.6 seconds to 5.7 seconds. For the range of test cases and test conditions, the ramp rates vary considerably, from -200 AMP/s to -64 AMP/s, depending on the power transfer initial condition. During a curtailment event, the steady-state power transfer (or AC current drawn) differs slightly from the requested curtailment. Most cases result with the power transfer or AC current draw slightly below the curtailment request; however, a few test cases result in up to 2.2% higher power transfer than the curtailment request.

This report also includes 100 kW wireless power transfer (WPT) EVSE characterization, including metadata or system specifications and the test results parameters. Metadata includes ground-side coil dimensions (x, y, or diameter in mm), vehicle-side coil dimensions (x, y, or diameter in mm), vehicle-side weight if known (kg), and standby active/reactive power consumption with no vehicle present (W/VAr), and the standby EM-field with no vehicle present (μT). Test results parameters include (1) the DC output power (kW) in perfectly aligned condition at nominal airgap, (2) operating frequency, (3) DC input to DC output efficiency (if measurable), (4) AC input to DC output efficiency (if a front-end rectifier is used), (5) efficiency at or near nominal power (%), (6) EM-field at 0.8m away from the center of the receiver coil in laboratory setups or EM-field at the edge of the vehicle body in vehicle integrated systems (closest approach boundary), (7) input power factor, (8) AC input voltage, and (9) input current total harmonic distortions (THD) in systems with front-end rectifiers. For the nominal operating conditions, nominal DC output power and efficiency at nominal power are recorded, and efficiency is characterized as a function of the output power with 10 kW or 10 AMP increments, whichever is possible, depending on the test conditions and the test equipment. The output may use resistive loads reflecting the nominal voltage range of the battery packs of the target vehicle platforms. Battery loads can be used at the output. Performance characterization for the off-nominal conditions involve several misalignment scenarios, including the $\Delta x = \pm 7.5$ cm longitudinal and $\Delta y = \pm 10$ cm lateral misalignments; angular misalignment conditions, including roll angle ($\Delta\Psi = \pm 2^\circ$), pitch angle ($\Delta\theta = \pm 2^\circ$), and yaw angle ($\Delta\phi = \pm 3^\circ$) misalignment conditions; and testing the system at another airgap condition that is different than the nominal airgap. Results show that the system efficiency is around 94.4% below nominal conditions at peak power of 100kW. Under nominal conditions, the wireless EVSE

demonstrated similar performance in lateral and longitudinal misaligned conditions, or their combination for up to 4 inches in any direction, with no significant drop in efficiency or power transfer (about 0.6% to 0.7% maximum drop in efficiency). Yaw, pitch, and roll angle misalignments also maintained the same power transfer rate and efficiency while the yaw angular misalignment slightly increased the efficiency. The electromagnetic and electric field emissions are also presented at required distances from the center of the couplers.

The EVSE characterization of high-power charging infrastructure presented in this report provides valuable data and results for use by numerous entities. This includes modeling and simulation organizations, decision makers, fleet planning, industry stakeholders, and many others involved with the development and deployment of electrified transportation technologies. Additional high-power conductive and wireless EVSE characterization results are anticipated from additional EVSE brands and models. These results will be reported on in future publications in support of the U.S. DOE EVs@Scale consortium Next-Gen Profiles project.

Table of Contents

Executive Summary	vi
1 EVSE Characterization Introduction	1
1.1 Conductive EVSE Characterization Hardware Configuration.....	1
1.2 Wireless EVSE Characterization Hardware Configuration	3
1.3 Measurement Parameters	4
1.3.1 Conductive EVSE Measurement Parameters.....	4
1.3.2 Metadata/System Parameters of the 100-kW Wireless EVSE.....	5
1.4 Measurement Locations	6
2 EVSE Characterization Testing Conditions and Procedures	9
2.1 Test Conditions	9
2.1.1 Conductive EVSE Test Conditions.....	9
2.1.2 Wireless EVSE Specific Test Conditions and Parameters	10
2.2 Test Procedures	11
2.2.1 EVSE Power Transfer Characterization at Nominal Conditions.....	11
2.2.2 EVSE High-Utilization Characterization.....	11
2.2.3 EVSE Characterization at Off-Nominal Ambient Temperature Conditions	13
2.2.4 EVSE Characterization at Off-Nominal Grid Input Conditions	13
2.2.5 EVSE Characterization during Smart Energy Management Curtailment.....	15
3 Conductive Power Transfer EVSE Characterization Results and Analysis	16
3.1 Nominal Test Conditions Results.....	16
3.2 High-Utilization Test Results.....	21
3.3 Off-Nominal Test Conditions Results.....	22
3.3.1 AC Voltage Deviation.....	22
3.3.2 AC Frequency Deviation	23
3.3.3 AC Harmonics Injection	23
3.4 OCPP Smart Energy Management Test Results	24
3.5 Summary of Conductive EVSE Characterization Results and Analysis.....	29
4 Wireless Power Transfer EVSE Characterization Results and Analysis.....	30
4.1 Nominal Operating Conditions Test Results.....	30
4.1.1 Efficiency Characterization Results.....	30
4.1.2 Electromagnetic Field and Electric Field Emissions	33
4.2 Off-Nominal Operating Conditions Test Results.....	35

List of Figures

Figure 1. EVSE Characterization Configuration.	2
Figure 2. EVSE2 In-laboratory installation.	3
Figure 3. (b) Experimental test setup and hardware for the 100-kW WPT EVSE system.	4
Figure 4. EVSE system topologies.	7
Figure 5. EVSE power cabinet AC power metering.	8
Figure 6. Charge dispenser DC and AC auxiliary power metering locations.	8
Figure 7. EVSE2_1 AC-to-DC steady-state efficiency.	17
Figure 8. EVSE2_1 power factor.	18
Figure 9. EVSE2_1 steady-state harmonic distortion on input current.	18
Figure 10. EVSE2_1 losses and auxiliary loads during 400 VDC power transfer.	19
Figure 11. EVSE2_1 losses and auxiliary loads during 850 VDC power transfer.	20
Figure 12. EVSE2_1 high-utilization test results at 750 VDC power transfer.	22
Figure 13. Response to OCPP curtailment request during 350 kW at 850 VDC power transfer.	25
Figure 14. Response to OCPP curtailment request during 500 AMP at 400 VDC power transfer.	26
Figure 15. Response to OCPP clear curtailment request during 350 kW at 850 VDC power transfer.	27
Figure 16. Response to OCPP clear curtailment request during 500 AMP at 400 VDC power transfer.	28
Figure 17. Efficiency characteristics of the system at nominal conditions for three different resistive load conditions as a function of output power.	30
Figure 18. Power analyzer screenshot for 1.9 Ohm load resistance at 100 kW nominal output power condition.	31
Figure 19. Efficiency characterization of EVSE7 at four battery voltages at different power levels.	32
Figure 20. System efficiency (94.44%) with 390 V battery voltage with 100 kW load power.	33
Figure 21. Electromagnetic field emissions as a function of distance from the center of the secondary coupler with 100 kW power transfer condition.	34
Figure 22. Electric field emissions as a function of distance from the center of the secondary coupler with 100 kW power transfer condition.	35
Figure 23. Off-nominal condition definitions with respect to coil positions.	36
Figure 24. $\Delta x=7.5\text{cm}$ and $\Delta y=10\text{cm}$ misalignment position from two different view angles.	37
Figure 25. Illustration of misaligned positions, including Δx and Δy misaligned positions and the power levels, achieved for each condition.	38
Figure 26. Efficiency map of the system under misaligned conditions.	39
Figure 27. Efficiency map of the system under misaligned conditions in contour lines.	40

Figure 28. System efficiency at 100 kW power transfer with 30° yaw angle rotational misaligned condition.	42
Figure 29. Coupling coils with increased airgap to 7 inches.	43
Figure 30. System efficiency at 100 kW power transfer with increased airgap condition.	43

List of Tables

Table 1. EVSE Characterization Measurement Parameters.	5
Table 2. Metadata and system parameters of EVSE7 characterized this study.	6
Table 3. EVSE power transfer characterization test conditions.	9
Table 4. EVSE characterization boundary conditions.	9
Table 5. EVSE high-utilization test sequence.....	12
Table 6. EVSE voltage deviation test.	14
Table 7. EVSE frequency deviation steps.....	14
Table 8. EVSE percent voltage harmonics injection steps.	15
Table 9. Phase-to-phase current imbalance during all steady-state power transfer tests.....	20
Table 10. Standby power consumption (no power transfer).....	20
Table 11. Impact of AC input voltage deviation on DC output current.	23
Table 12. Impact of AC frequency deviation on DC output current.	23
Table 13. Impact of 5% AC voltage harmonics on DC output current.....	23
Table 14. Curtailment latency and ramp rates for OCPP curtailment requests.	24
Table 15. Curtailment latency and ramp rates for OCPP clear curtailment requests.	24
Table 16. Steady-state power transfer characteristics during OCPP curtailments.....	28
Table 17. Steady-state power transfer characteristics during OCPP curtailments.....	29
Table 18. System performance under all nominal and off-nominal conditions.....	41

1 EVSE Characterization Introduction

This report provides data and results from the conductive and wireless charging electric vehicle supply equipment (EVSE) characterization study performed for the U.S. DOE EVs@Scale Next-Gen Profiles project, which aligns with other three reports from this project: High-Level Analysis report, EV Profile Capture report, and Fleet Analysis report.

The characterization of high-power charging infrastructure is crucial for ensuring the reliability, interoperability, and efficiency of the electric vehicle (EV) charging ecosystem. The thoroughness of this characterization involves the exploration/comparison of production and future charging equipment, which include conductive and non-conductive (wireless power transfer, WPT) EVSE systems, respectively. Using EV emulators, EVSE can be tested under controlled conditions that are both repeatable and consistent, simulating the diversity of EV characteristics to be expected in production DC fast charging. Performing these tests in a controlled environment allows for potential issues, optimizations, design improvements, and testing strategies to arise, ultimately fostering a more robust and user-friendly infrastructure for electric vehicles. This paper focuses on the characterization of EVSEs with respect to power and system efficiency at different boundary conditions and focuses less on interoperability and reliability.

This paper's research of conductive and non-conductive charging systems characterization was performed using a wide range of DC output current and DC voltage charging conditions to quantify the operational performance of the EVSE. This characterization was conducted at nominal or off-nominal test conditions. Conductive EVSE characterization aims to explore performance across boundary conditions pertaining to ambient temperature, AC grid input conditions, and Smart Energy Management system curtailment requests. Additionally, high-utilization testing was conducted to quantify the EVSE performance during quick succession, short-duration charge sessions at full power. For WPT, nominal cases for the previous conditions are used; however, an additional set of WPT-specific boundary conditions are explored pertaining to misalignment and airgap scenarios between the EVSE and EV emulator coils.

The test article nomenclature in these reports is aligned for cross-report comparison. For example, EVSE2_1 refers to EVSE#2 operating on the CCS-1 liquid-cooled cable, which is the first of two charge dispenser cables. EVSE2_2 refers to EVSE#2 operating on the second cable, which is CHAdeMO. EVSE7 refers to the EVSE#7 operating via a WPT coil. Characterization of the CHAdeMO charging connector is not evaluated in the Next-Gen Profiles project.

1.1 Conductive EVSE Characterization Hardware Configuration

EVSE characterization testing is intended to test an EVSE at a single port. Multi-port/multi-session EVSE is not included in the completed characterization. Figure 1 depicts the configuration for

EVSE characterization, including the EVSE power cabinets, EVSE dispenser, and an EV emulator load. EV emulator use enables repeatable testing across a wide range of voltage test conditions and accelerates testing by alleviating the time to discharge the battery energy storage system associated with an EV used for EVSE testing. For the EVSE characterization, the EVSE system is considered to be the device under test. The EVSE is not modified out of the standard commercial configuration and settings of the manufacturers. The EVSE are instrumented to capture the metrics detailed in Table 1. The locations of the measurement points are described in subsequent sections.

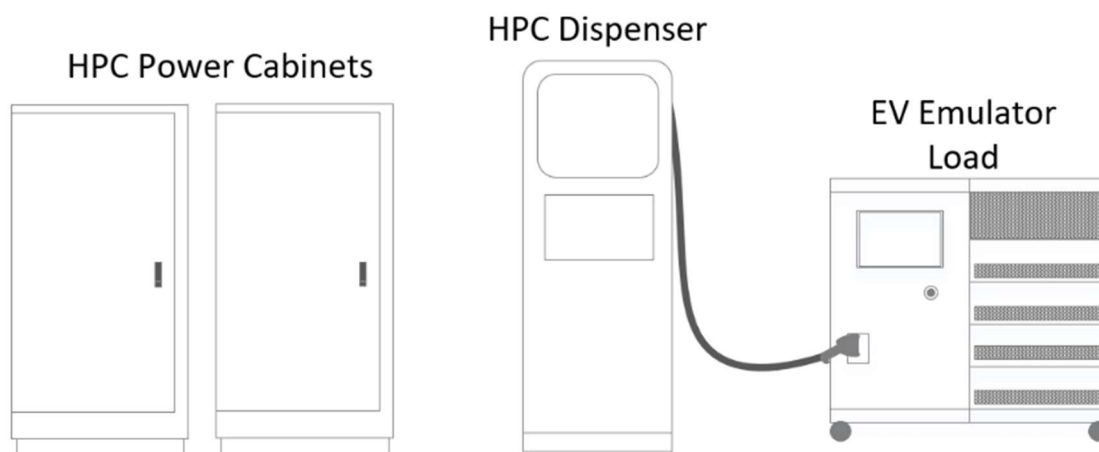


Figure 1. EVSE Characterization Configuration.

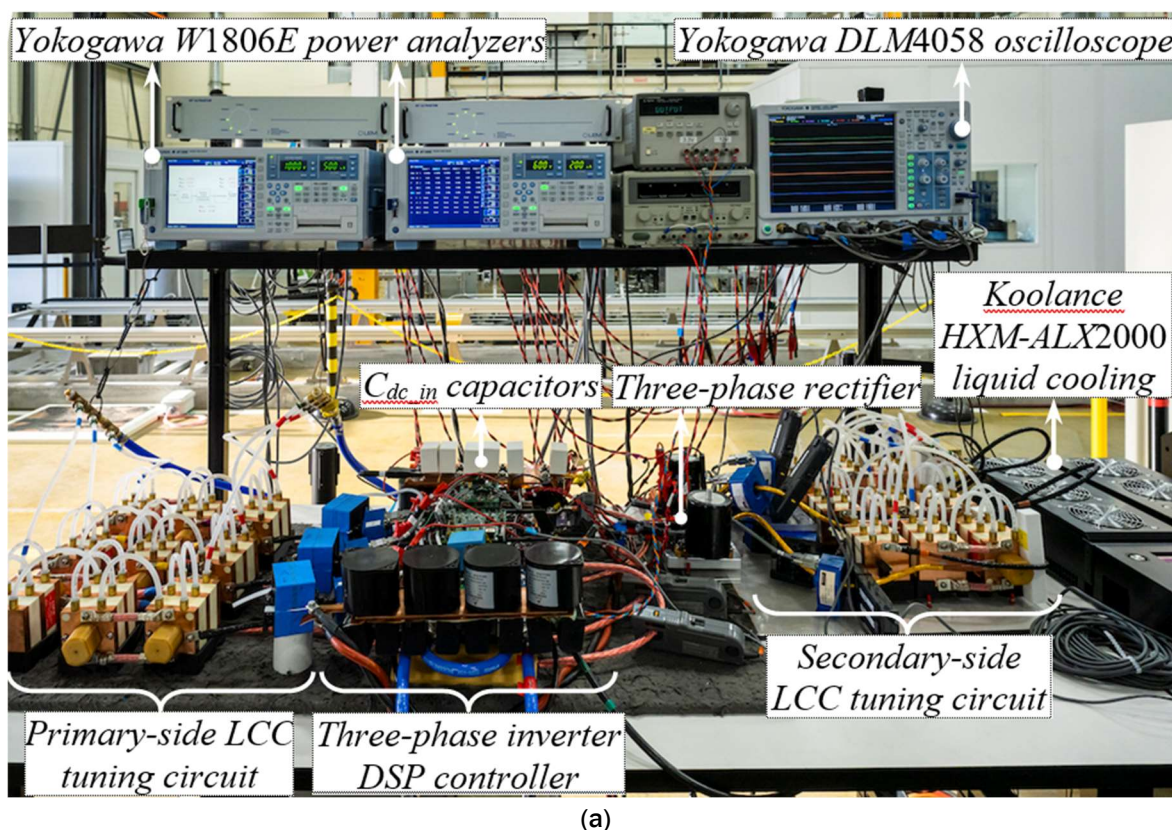
EVSE2 is comprised of two power cabinets and one dispenser equipped with one CCS-1 liquid-cooled cable and one CHAdeMO cable. EVSE2 is installed in a laboratory setting as a temporary installation on metal support structures to support the EVSE enclosure size and mass and to enable the installation of the necessary wiring without modifying the concrete floor of the laboratory space. The AC input wiring consists of 4/0 AWG type-W single conductor cables from the 480 VAC service disconnect to each of the two power cabinets. The DC wiring from each power cabinet to the dispenser cabinet is MCM 350 type-W single conductor cables. Additionally, two AWG type-W cables are used to bond the cabinets to the ground at the electrical service disconnect. The cable lengths range from 10–15 feet in length for the AC and DC cabling. The EVSE support structure and the wiring between the enclosures are shown in Figure 2.



Figure 2. EVSE2 In-laboratory installation.

1.2 Wireless EVSE Characterization Hardware Configuration

The test setup for EVSE7 characterization work is provided in Figure 3 in which the power electronics system hardware and test equipment are shown in Figure 3(a) while Figure 3(b) shows the 300-kW rated transmitter, the 100-kW receiver couplers, and additional hardware and their connections. The test setup uses two 6-channel Yokogawa high-precision power analyzers and two 8-channel oscilloscopes and load and source emulators to power and load the system while recording the data.



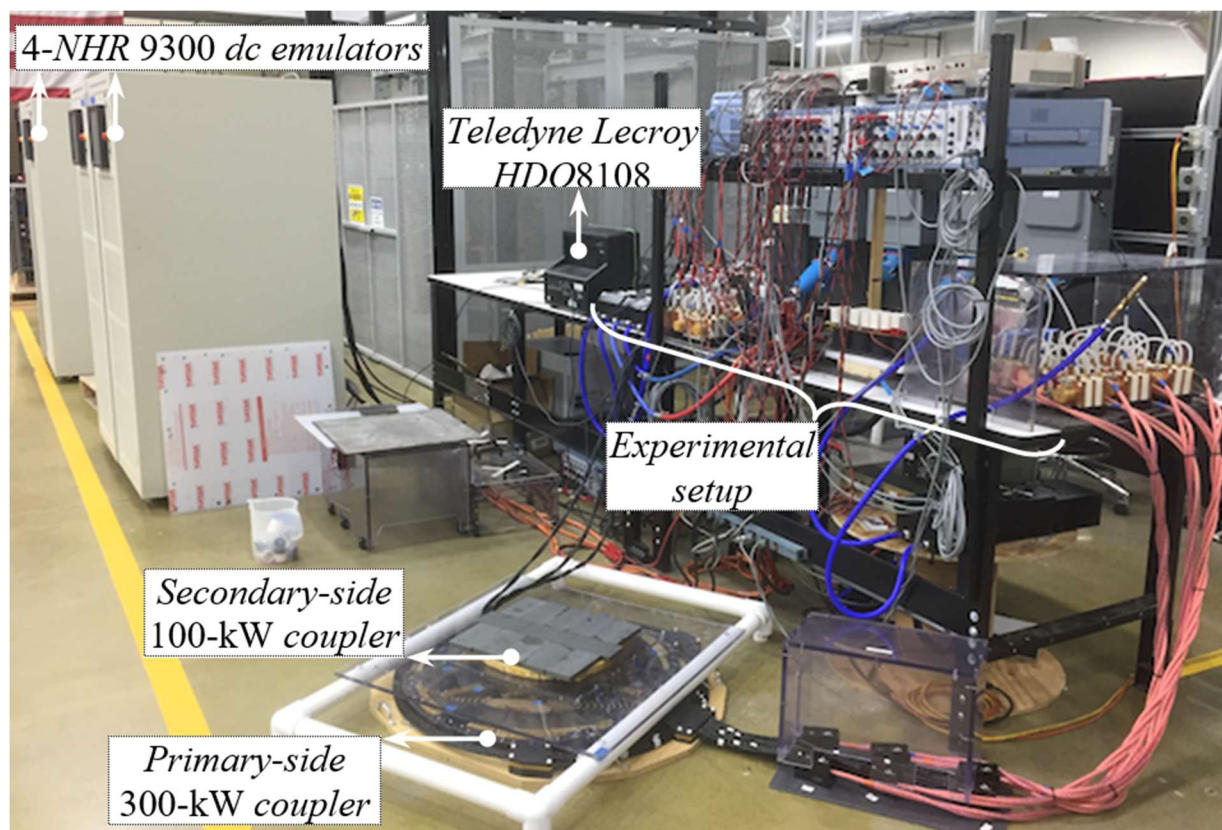


Figure 3. (b) Experimental test setup and hardware for the 100-kW WPT EVSE system.

1.3 Measurement Parameters

1.3.1 Conductive EVSE Measurement Parameters

For EVSE characterization, approximately 30 parameters are collected using power analyzers and other laboratory-grade sensors to quantify and characterize the system operation. It should be noted that many of the same measurement parameters are similarly described in “EV Profile Capture: A Next-Gen Profiles Project Report.” These measurements are harmonized with the EV charge profile measurements and are further supported by the addition of a few parameters enabled by using an EV emulator. A few vehicle-specific parameters, such as battery temperature, are omitted as they do not apply to EVSE characterization. Table 1 details the EVSE characterization parameters. The EVSE Unique ID, firmware, and software version parameters have been omitted, or altered, for anonymity. The Energy Management Source Curtailment Request is only recorded for sessions that are performed with Smart Charge Management (SCM) testing.

Table 1. EVSE Characterization Measurement Parameters.

Measurement Location	Parameter	Phase	Units
Metadata	EVSE Unique ID	-	-
	EVSE Firmware/Software version	-	-
	Vehicle emulator model / information	-	-
	Vehicle emulator ID	-	-
	Timestamp	-	MM/DD/YY hh/mm/ss.dd
480 VAC Input to each Power Cabinet	Voltage	A, B, C	V (RMS)
	Current	A, B, C	A (RMS)
	Frequency	A	Hertz
	Real Power	A, B, C	kW (RMS)
	Reactive Power	A, B, C	kVAR (RMS)
	Apparent Power	A, B, C	kVA (RMS)
	Power Factor	-	-
	Current THD	A, B	%
	Current Harmonics	3rd, 5th, 7th, 9th	-
Ambient Temperature	Temperature	-	°C
Energy Management Source	OCPP Server/E-mobility service provider, other	-	Curtailed request A or kW
Vehicle Inlet Port	Voltage	DC	V
	Current	DC	A
	Power	DC	kW
EVSE Charge Pedestal Output	Voltage	DC	V
	Current	DC	A
	Power	DC	kW
	DC current ripple	DC	%
EVSE Auxiliary System(s)	Voltage	DC	V
	Current	DC	A
	Power	DC	kW
EVSE CCS Cable	CCS cable temperature	-	°C
EVSE CCS Connector	CCS connector temperature	-	°C
EVSE Power Cabinet	Power cabinet internal air temperature	-	°C

1.3.2 Metadata/System Parameters of the 100-kW Wireless EVSE

Metadata and system parameters of the 100-kW wireless EVSE system is provided in Table 2, including the rated power, diameter, wire configuration, weight, wire thickness, airgap, operating

frequency, and coil-to-coil efficiency at nominal conditions. the transmitter is designed for a 300-kW power rating, while the receiver featured in this characterization work is rated for 100 kW. In the future, this system will also be tested with a 270-kW rated receiver coupler, and the system will be characterized with those couplers.

Table 2. Metadata and system parameters of EVSE7 characterized this study.

Parameters	Primary Coupler	Secondary Coupler
Rated power [kW]	300	100
Diameter [mm]	750	375
Wire configuration	4 AWG, 3 wires/phase	4 AWG, 1 wire/phase
Copper mass [kg]	9.9	2.4
Ferrite mass [kg]	32.3	6.4
Total weight [kg]	42.2 +10 kg for auxiliary parts	8.8 + 6.3 kg for auxiliary parts
Litz wire thickness [mm]	8.6	8.6
Ferrite thickness [mm]	15	20
Copper losses [W]	697	169
Ferrite losses [W]	1665	311
Airgap [inches]	5 inches nominal	
Operating frequency [kHz]	83	
Coil-to-coil efficiency [%]	97.4	

1.4 Measurement Locations

This section describes the locations of the measurements taken for each parameter detailed in the previous section. To produce consistent measurements across multiple charger topologies, the measurement locations for each topology under test are explicitly defined. This measurement location definition is consistent for the EV charge profile measurements and the EVSE characterization measurements. Figure 4 depicts the two types of conductive charger topologies used in the Next-Gen Profiles project: paralleled at the dispenser and primary power cabinet. On the left of Figure 4, each power cabinet is DC-coupled directly to the EVSE dispenser; this is considered a paralleled system that is coupled at the dispenser. In the image on the right of the figure, the power cabinets system only has a single DC connection to the dispenser; this is considered a paralleled system that is coupled at the primary cabinet. This difference in topology drives the requirements on the measurement locations for each system to properly characterize the power flow within the charging system.

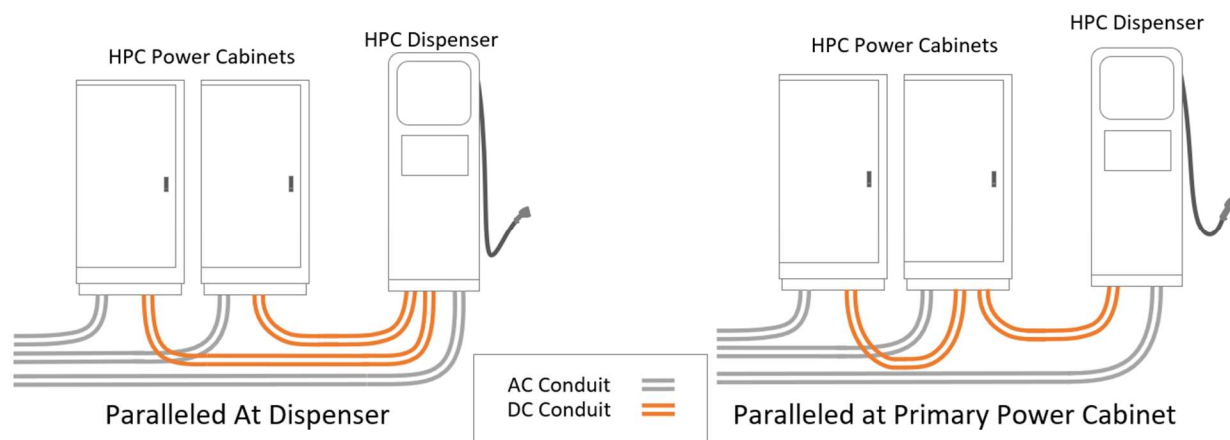


Figure 4. EVSE system topologies.

The AC electrical input to the HPC EVSE is measured at the input to each power cabinet as supplied from (downstream of) the local service panel, as shown in Figure 5. For three phase measurements, the two-wattmeter method was employed for some of the charge sessions, and direct measurements of all three phases were also used. The DC output from the EVSE was measured at the EVSE dispenser and at the EV inlet port of the EV emulator.

The auxiliary system measurements in the HPC EVSE include cooling, controls, lighting, and front touch panels among other loads. These measurements are made at the EVSE source location. The DC output and the AC auxiliary power measurement locations at the dispenser are shown in Figure 6.

The temperature measurements for the cable and connector temperatures are obtained from the cable manufacturer's installed thermistors within the CCS cable and CCS connector. The cable temperature sensor is at the surface of the coolant system tubing inside the charge cable. The CCS connector temperature sensor is located inside the CCS connector adjacent to the DC pins in the CCS connector. The EVSE power cabinet's internal air temperature is obtained by a manufacturer-installed temperature sensor inside each of the power cabinets.

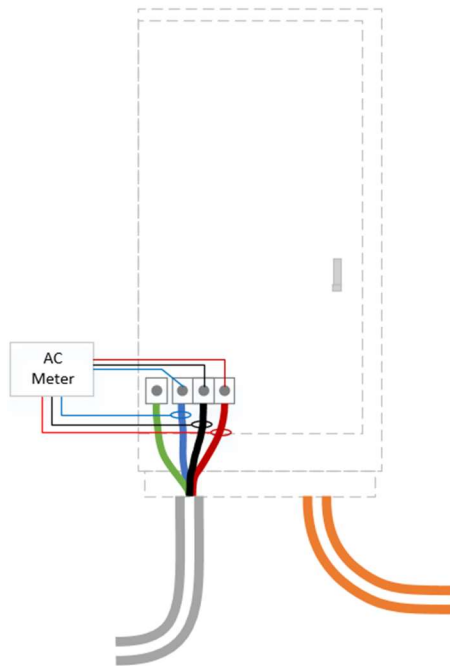


Figure 5. EVSE power cabinet AC power metering.

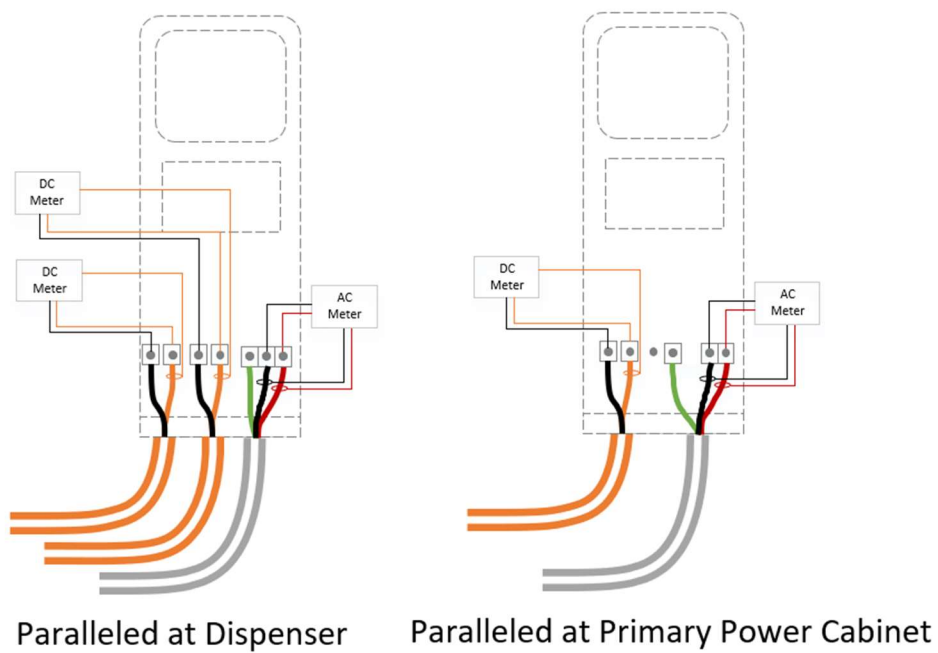


Figure 6. Charge dispenser DC and AC auxiliary power metering locations.

2 EVSE Characterization Testing Conditions and Procedures

2.1 Test Conditions

2.1.1 Conductive EVSE Test Conditions

During EVSE characterization, DC current and DC voltage measurements are made to quantify the operational performance of the EVSE over a wide range of EVSE power transfer conditions. Off-nominal ambient temperature, grid input voltage characteristics, EVSE utilization duty-cycle, and WPT misalignment testing conditions are collected to characterize the full set of expected real-world operating conditions. Table 3 details the DC power transfer conditions during nominal and off-nominal test conditions.

Table 3. EVSE power transfer characterization test conditions.

Test Condition Category	DC Current Test Conditions	DC Voltage Test Conditions	Tolerance
Nominal test conditions	50 to 500 AMP in 10A increments (up to maximum power)	300 V, 400 V, 650 V, 750 V, 850 V	+/-2%
Off-nominal test conditions	150 AMP, 500 AMP (or full power if 500 AMP is not possible)	400 V, 850 V	+/-2%

The test boundary conditions for EVSE characterization of nominal and off-nominal test conditions are detailed in Table 4, including off-nominal ambient temperature conditions, AC grid input conditions, and smart energy management request details. The parameters highlighted in green are the test conditions for the nominal test conditions for EVSE characterization.

Table 4. EVSE characterization boundary conditions.

Condition Category	Condition Sub-Category	Condition Metric	Tolerance
WPT Alignment	X-Direction	Aligned (<5% coil length offset)	
		10% coil length offset	+/- 2%
		25% coil length offset	+/- 2%
		40% coil length offset	+/- 2%
	Y-Direction	Aligned (<5% coil length offset)	
		10% coil length offset	+/- 2%
		25% coil length offset	+/- 2%
		40% coil length offset	+/- 2%

	Z-Direction	Unloaded Vehicle	+/- 50mm from nominal air gap
Temperature	Ambient Temperature	Nominal: 23 °C	+/- 2%
		Hot: 40°C	+/- 2%
		Cold: -7°C	+/- 2%
Grid Condition	Voltage	Nominal: 480VAC	+/-25VAC
		Swelled: 528VAC (110% nominal)	+/-25VAC
		Sagged: 432VAC (90% nominal)	+/-25VAC
	Harmonics	Nominal: No Harmonics	
		5% Voltage Distortion	+/- 1%
	Frequency	Nominal: 60 Hz	+/- 0.2 Hz
		Increased: 61.2 Hz	+/- 0.2 Hz
		Decreased: 58.8 Hz	+/- 0.2 Hz
Charge Management	Smart Charge Request	Nominal: None	-
		<i>TxProfile</i>	-
		<i>TxDefaultProfile</i>	-
		<i>ChargePointMaxProfile</i>	-
	Smart Charge Request Duration	Nominal: None	-
		2 minutes	+/- 1 minute
	Smart Charge Request Scheduling	Nominal: None	-
		1 minute into charge session	-
	Current or Power Request	Nominal: None	-
		65A (total AC input current)	-
		54kW (AC or DC as implemented by manufacturer)	-

A nominal test is conducted under ideal conditions that should transfer the maximum allowable energy in the shortest amount of time possible. The following EVSE parameters must be fulfilled to complete a nominal test: (1) outside ambient temperature must be 23°C, (2) smart charge values must all be FALSE, and (3) no limits should be placed on the EVSE cabinets or available DC current.

2.1.2 Wireless EVSE Specific Test Conditions and Parameters

The project team has worked on standardized test procedures on WPT-based EV charging systems (wireless EVSEs) for nominal and off-nominal test conditions. The “EVSE Characterization Recommended Test Procedures for WPT Systems” document functions as the guide to complete the EVSE7 characterization, including the metadata and results parameters. The efficiency data was collected in 10 kW increments for both resistive load and battery load conditions. This covered the full range of the load resistance and full range of the battery voltage (i.e., 300–400 V). The nominal conditions represent nominal z-gap and perfectly aligned transmitter and receiver coils with zero yaw, roll, and pitch angles. Off-nominal conditions include change in nominal z-gap and misaligned conditions for $\Delta x = \pm 7.5\text{cm}$ while $\Delta y = 0$ and $\Delta y = \pm 10\text{cm}$ while $\Delta x = 0$ and combination

worst-case misalignment of $\Delta x = \pm 7.5\text{cm}$ and $\Delta y = \pm 10\text{cm}$. The other off-nominal conditions as per SAE J2954 include yaw angle of $\Delta\Phi = \pm 3^\circ$, roll angle of $\Delta\phi = \pm 2^\circ$, and pitch angle of $\Delta\theta = \pm 2^\circ$.

2.2 Test Procedures

EVSE characterization requires detailed planning, preparation, and execution to successfully acquire accurate and meaningful results for the testing program. This section describes the test procedures and setup requirements for the numerous areas of EVSE characterization.

2.2.1 EVSE Power Transfer Characterization at Nominal Conditions

Measurement parameters are collected across a wide range of DC current and DC voltage test points (quasi-steady-state testing) at nominal test conditions, as detailed in Table 3. The test procedures and requirements for the quasi-steady-state testing are as follows:

- The EVSE will soak at the ambient temperature prescribed for the test conditions for a minimum of four hours prior to the test's commencement.
- The charge session can be continuous for the numerous test points of the quasi-steady-state testing, or the test operator may end the charge session and begin a new charge session as necessary. The EVSE does not need to soak for four hours at ambient temperature again prior to resuming steady-state testing.
- Record the vehicle emulator make/model, EVSE make/model /firmware version, ambient temperature, day/time.
- Data measurements are collected at a rate of 10 Hz.
- Each quasi-steady-state DC current and DC voltage test point is held for a minimum of 180 seconds. This is necessary to ensure the EVSE reaches steady-state operation.
 - Steady state is defined as ± 0.2 ADC and ± 1 VDC over the final 30 seconds of the 180-second sample period.
- The final 30 seconds of collected data are averaged to determine a single steady-state value for each measurement parameter for each quasi-steady-state test point.

2.2.2 EVSE High-Utilization Characterization

EVSE characterization during repetitive or high-utilization power transfer sessions is conducted to determine the EVSE operational characteristics and power consumption of the EVSE auxiliary control systems. Of particular interest is the CCS liquid-cooled cable thermal management system. Three full-power, 10-minute charge sessions are conducted consecutively, with a small rest period between each charge session. This test sequence is representative of three EVs charging consecutively at one EVSE, with little time between charge session. Each charge session is conducted at 750 VDC and 500 AMP (or full power if the EVSE is not capable 500 AMP at the required voltage). In between each charge session the charge cable is unplugged from the EV

emulator and returned to the cable holster on the EVSE charge dispenser. Measurements are taken continuously throughout all seven consecutive test steps as detailed in Table 5.

Table 5. EVSE high-utilization test sequence.

Step #	Duration	Test Condition Category	DC Current Test Conditions	DC Voltage Test Conditions	Tolerance
1	30 s	Plug in and start charge session	Ramp up current to Step #2		+/-30 s
2	10 min.	Steady-state power transfer	500 AMP request	750 V	+/-2%
3	240 s	Stop charge session, unplug	0A		+/-30 s
4	10 min.	Steady-state power transfer	500 AMP request	750 V	+/-2%
5	240 s	Stop charge session, unplug	0A		+/-30 s
6	10 min.	Steady-state power transfer	500 AMP request	750 V	+/-2%
7	30 s	Stop charge session, unplug	0A		+/-30 s

- The EVSE will soak at the ambient temperature prescribed for the test conditions for a minimum of 4 hours prior to commencing testing.
- Record the vehicle emulator make/model, EVSE make/model /firmware version, ambient temperature, day/time, etc.
- Data collection of the measurement parameters must be continuous through the entire test sequence:
 - Begin data collection at least 5 seconds prior to plugging the EVSE into the EV emulator.
 - Continue data collection for at least 5 seconds after unplugging the EVSE from the EV emulator.
- Data measurements will be collected at a rate of 10 Hz.
- The EVSE high-utilization characterization test sequence must be continuous and uninterrupted, as detailed in Table 5.
- Test steps must be conducted in the order detailed in Table 5. The order of the test steps cannot be changed.
- Do not clear, reset, or reboot any portion of the EVSE or alerts displayed by the EVSE during the test sequence.
 - Take note of any alerts or errors from the EVSE during the test sequence, as part of the data collected.

- If the EVSE is not capable of providing the requested DC current at the specified DC voltage, operate the EVSE at the highest DC current possible at the specified DC voltage test condition.
- After completing the entire test sequence, the EVSE may be rebooted or reset as necessary.

2.2.3 EVSE Characterization at Off-Nominal Ambient Temperature Conditions

Since ambient temperature can potentially impact the performance characteristics of the EVSE, quasi-steady-state testing is conducted at two off-nominal ambient temperature conditions (detailed in Table 4) across the range of DC current and DC voltage power transfer test points detailed in Table 3. The test procedures detailed below are similar to the test procedures for the nominal temperature steady-state testing to ensure the validity of the off-nominal temperature conditions:

- The EVSE will soak at the ambient temperature prescribed for the test conditions for a minimum of 4 hours prior to commencing testing.
- Record the vehicle emulator make/model, EVSE make/model /firmware version, ambient temperature, day/time, etc.
- Adhere to the test procedures detailed in the “EVSE Power Transfer Characterization at Nominal Conditions” section.

2.2.4 EVSE Characterization at Off-Nominal Grid Input Conditions

EVSE off-nominal AC grid input characterization is conducted using an AC grid emulator to create the AC input test conditions listed in Table 4. These conditions include voltage deviation, frequency deviation, and voltage harmonics injection. The voltage deviation and frequency deviation test conditions include both sag and swell conditions. Each of the test conditions is characterized independently; no concurrent off-nominal conditions are evaluated. Each off-nominal AC grid input test condition will be conducted at the off-nominal DC current and DC voltage power transfer test conditions detailed in Table 3.

The test procedures and requirements for the off-nominal AC input grid conditions testing are as follows:

- The EVSE will soak at the ambient temperature prescribed for the test conditions for a minimum of 4 hours prior to commencing testing.
- Record the vehicle emulator make/model, EVSE make/model /firmware version, ambient temperature, day/time, etc.
- Data measurements will be collected at a rate of 10 Hz throughout the test sequence.
- The charge session will be initiated at nominal AC input grid conditions.

- Each DC current and DC voltage test point is collected per the off-nominal condition tests of Table 3.
 - Acceptable tolerance for the power transfer prior to entering the off-nominal conditions is +/- 0.2 A and +/-1 V.

The off-nominal condition tests will be performed in accordance with Table 6 for AC voltage deviation testing, Table 7 for AC frequency deviation testing, and Table 8 for AC voltage harmonics injection testing.

Table 6. EVSE voltage deviation test.

Step #	% of Nominal	Voltage L-L (RMS)	Duration (second)
1	100%	480.0	20
2	98%	470.4	3
3	96%	460.8	3
4	94%	451.2	3
5	92%	441.6	3
6	90%	432.0	60
7	92%	441.6	3
8	94%	451.2	3
9	96%	460.8	3
10	98%	470.4	3
11	100%	480.0	20
12	102%	489.6	3
13	104%	499.2	3
14	106%	508.8	3
15	108%	518.4	3
16	110%	528.0	60
17	108%	518.4	3
18	106%	508.8	3
19	104%	499.2	3
20	102%	489.6	3
21	100%	480.0	20

Table 7. EVSE frequency deviation steps.

Step #	% of Nominal	Frequency (Hz)	Duration (sec)
1	100	60.0	20
2	99	59.4	3
3	98	58.8	3
4	99	59.4	3
5	100	60.0	3

6	101	60.6	3
7	102	61.2	3
8	101	60.6	3
9	100	60.0	20

Table 8. EVSE percent voltage harmonics injection steps.

Step #	% Voltage THD Injection	Duration (sec)
1	0.0%	60
2	5.0%	10
3	0.0%	30

- The charge sessions can be continuous for the numerous test points of the testing, or the test operator may end the charge session and begin a new charge session as necessary between each off-nominal test.

2.2.5 EVSE Characterization during Smart Energy Management Curtailment

Testing is conducted for EVSE smart charge management profile response using OCPP 1.6 or newer for the current and voltage test conditions of Table 4. The smart energy management curtailment requests include *ChargePointMaxProfile*, *TxDefaultProfile*, and *TxProfile*, which are used for curtailment requests of 54 kW and 65 AMP for a total of six curtailment profiles during the four DC power transfer test conditions as detailed in Table 3. Per the OCPP specification, the current curtailment requests are defined as the input to the EVSE (i.e., AC current); whereas the power curtailment requests are manufacturer specific at either the input or the output of the EVSE (i.e., AC input power or DC output power). The test procedures and requirements for the smart charge management characterization are as follows:

- Record the vehicle emulator make/model, EVSE make/model /firmware version, ambient temperature, day/time, OCPP server version, etc.
- Begin a charge session and operate the EVSE at the DC voltage and DC current values detailed in Table 4 off-nominal test conditions for a minimum of 60 seconds.
- Transmit the Table 4 smart charging profile request via OCPP 1.6 or newer (e.g., *TxProfile* 65 AMP current request):
 - If using charge management system alternatives that do not use OCPP, please note the system (e.g., local controller, cloud system) and specific signal request.
- After the Table 4 smart charge test is completed, use the *ClearChargingProfile* command to end the smart charge request.
- Once the charge profile request is accepted, allow EVSE to return to steady-state operation before ending data collection or continuing to the next test point.

- Repeat this test sequence for each DC current and DC voltage condition listed in Table 3 for each of the six smart energy management curtailment requests listed in Table 4.

3 Conductive Power Transfer EVSE Characterization Results and Analysis

Performance metrics and results are quantified from the EVSE characterization data collected from EVSE2_1, which refers to power transfer using the first cable (CCS-1) on EVSE2. Quantified values include power transfer capabilities, power transfer efficiency, AC power quality, AC phase imbalance, auxiliary and subsystem loads and losses, and component temperatures among others. During select tests, the real power and reactive power of the EVSE are measured before and after charging sessions to determine the standby consumption of the EVSE. This section describes the results of EVSE characterization during nominal and off-nominal test conditions.

3.1 Nominal Test Conditions Results

The nominal test conditions quasi-steady-state efficiency, power factor, and current total harmonics distortion performance results for EVSE2_1 are shown in Figure 7 to Figure 9. These results include the five DC voltage test conditions and cover the power transfer conditions from 50A DC to full current capability.

As seen in Figure 7, EVSE2_1 power transfer efficiency is >92% when AC input power is >50 kW. For power transfer at 650 VDC or higher, the power transfer efficiency is >93.5% when charging at AC input power is >75 kW. Overall, the peak efficiency of EVSE2_1 is >95% when operating at 750 VDC output and between 125 kW and 225 kW AC input power.

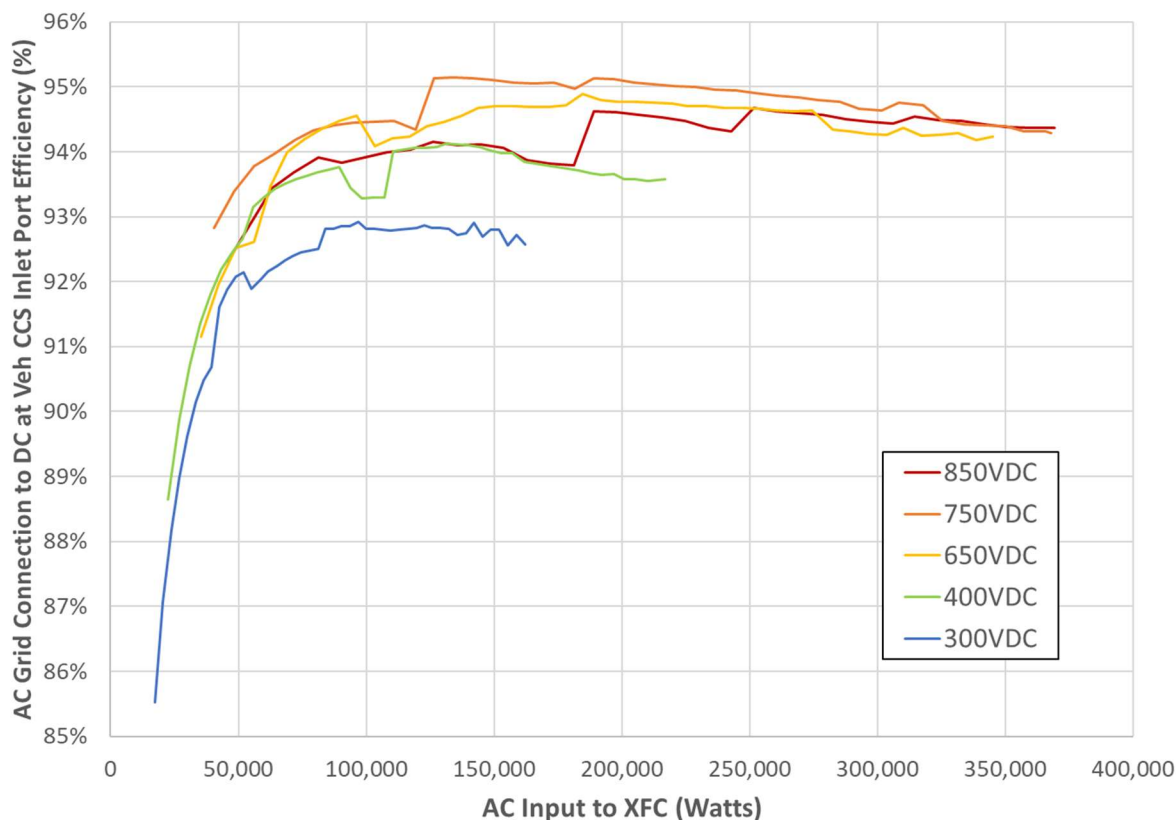


Figure 7. EVSE2_1 AC-to-DC steady-state efficiency.

The measured power quality characteristics of EVSE2_1 is illustrated in Figure 8 and Figure 9. The power factor of EVSE2_1 is >0.91 for power transfer above 50 kW AC input and has a maximum power factor of 0.975 when operating above 125 kW AC input, except for when 850 VDC is operating below 180 kW AC. The AC current harmonics produced by the EVSE2_1 is $<25\%$ for AC input power of >50 kW and is $<10\%$ for AC input power >180 kW. From these power quality results, it is noted that the power factor and current total harmonics distortion results show a dual trending patterns with respect to AC input power. This is due to the coordinated control of the dual power cabinets in which the two cabinets are not loaded equally or one cabinet is idle, therefore resulting in a discontinuous trend for the power quality results.

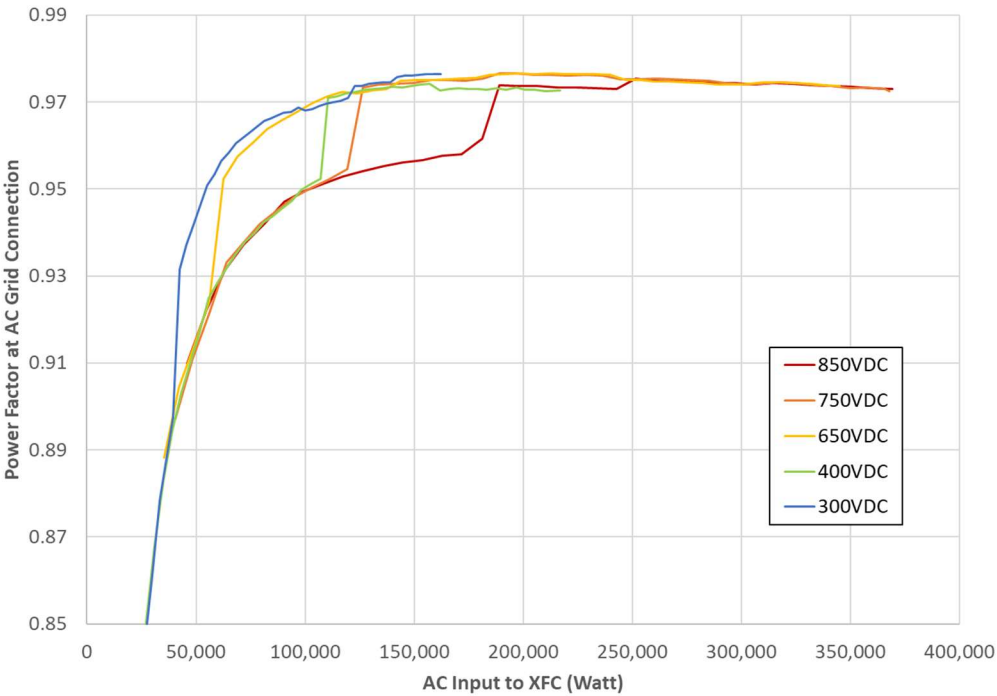


Figure 8. EVSE2_1 power factor.

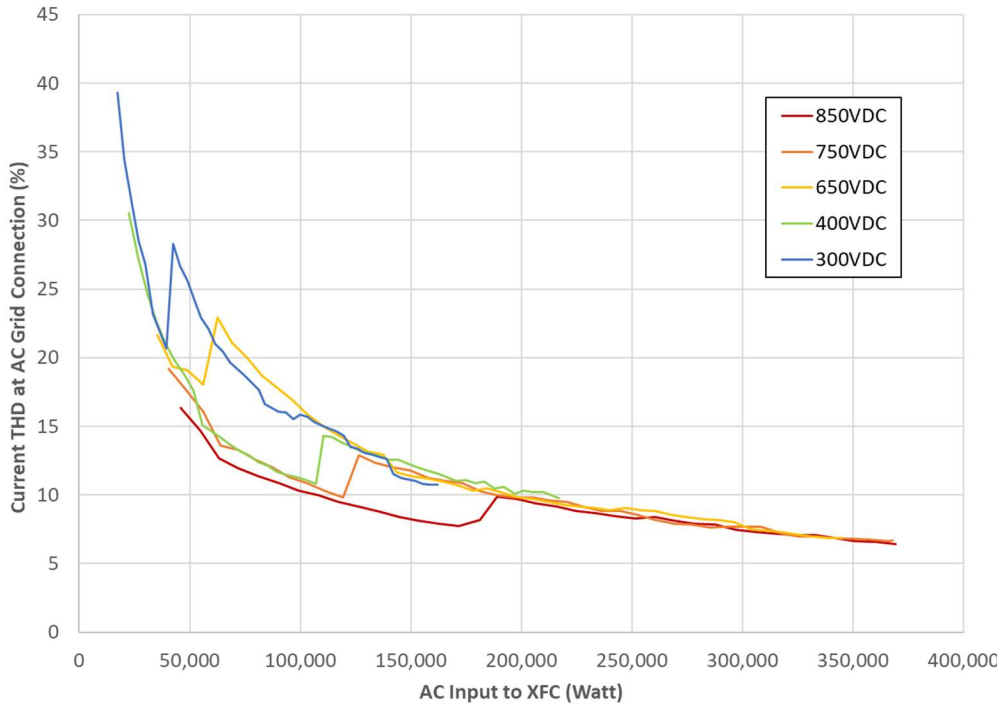


Figure 9. EVSE2_1 steady-state harmonic distortion on input current.

EVSE losses are quantified from the quasi-steady-state test conditions, and the results are shown for the 400 VDC and 850 VDC test conditions in Figure 10 and Figure 11, respectively. For both DC voltage test conditions, the EVSE losses are primarily due to AC-to-DC power conversion losses. These losses account for approximately four times more losses than the other EVSE losses combined. As shown in Figure 10, at full current (500A), the cable resistive losses and all auxiliary systems power draw (which includes the cable thermal management systems) are <2.5 kW, which impacts overall EVSE efficiency by <1.25%. The liquid-cooled cable in EVSE2_1 is rated for operation at 400 ADC and peak of 500 ADC. This cable is a 10-foot Huber+Suhner Radox HPC 400 HFFR 1000 V cable comprised of liquid-cooled DC conductors that appear to be smaller than 4 AWG. The gauge of the wiring cannot be determined without removing (and likely destroying) the coolant jacket around the conductor's electrical insulation.

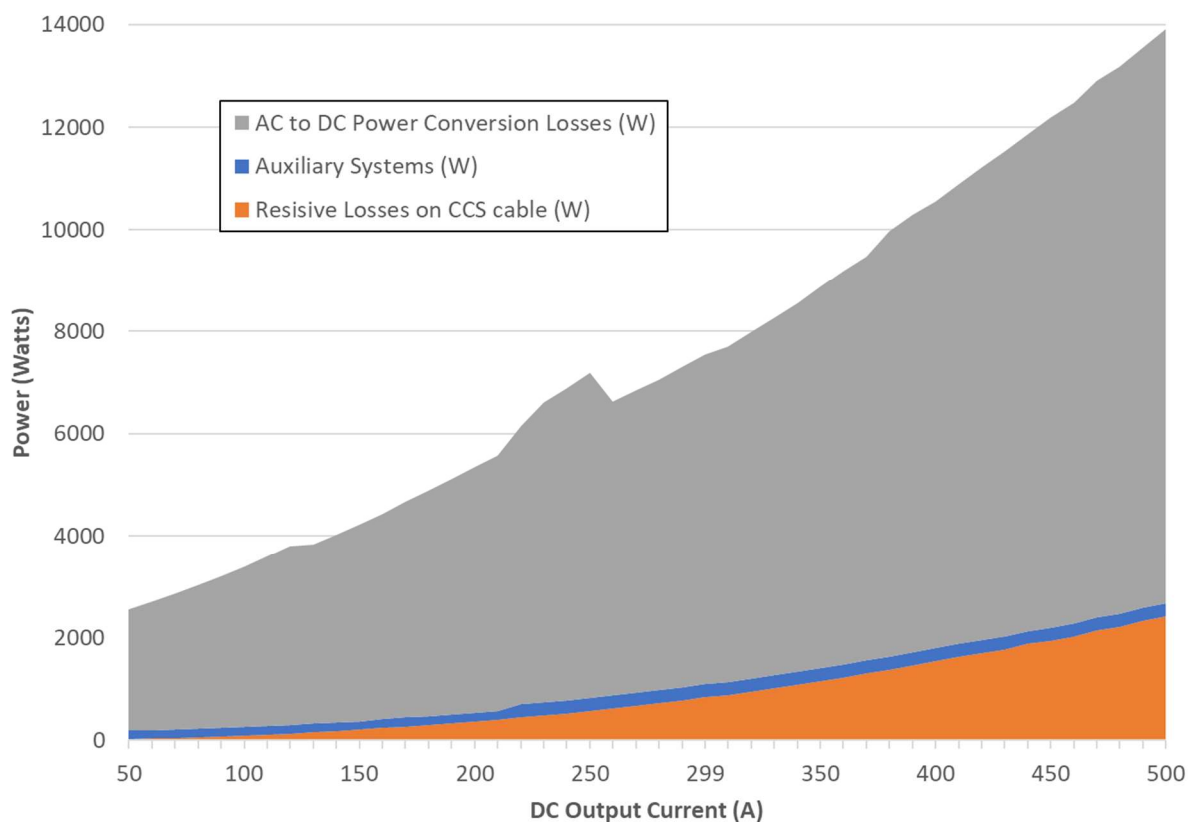


Figure 10. EVSE2_1 losses and auxiliary loads during 400 VDC power transfer.

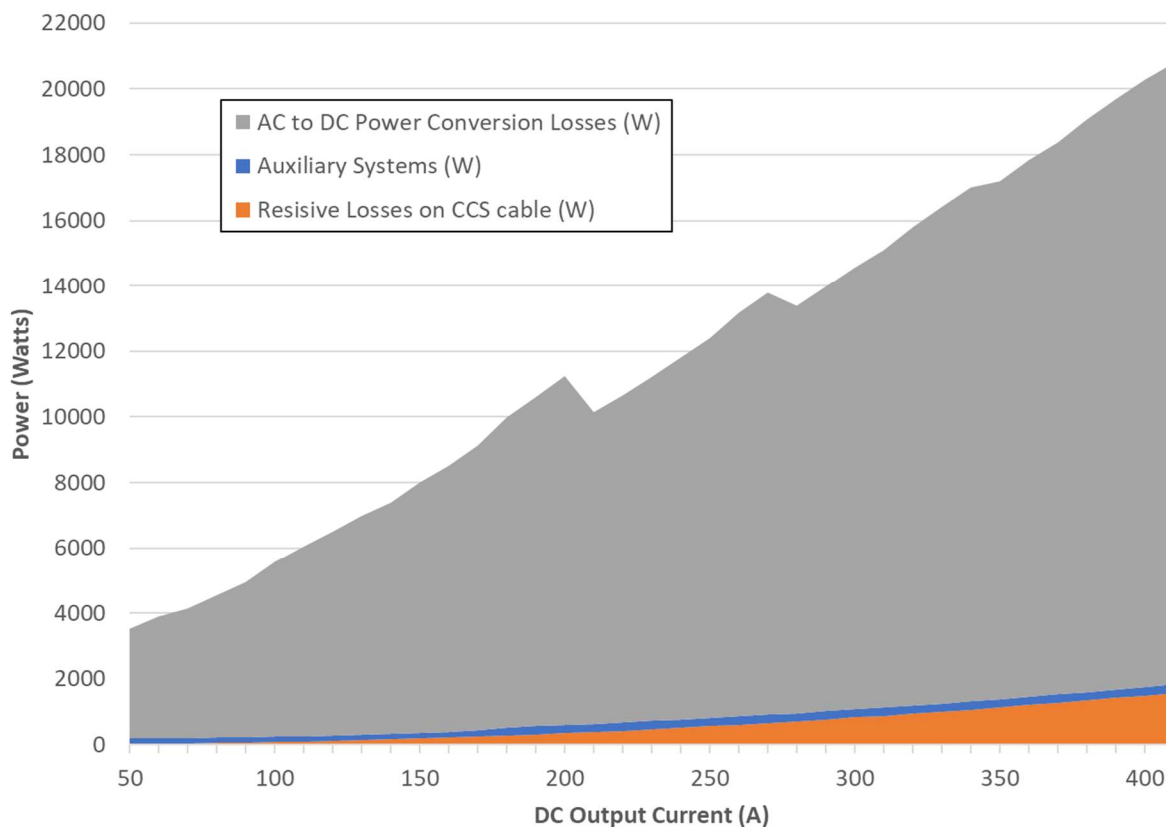


Figure 11. EVSE2_1 losses and auxiliary loads during 850 VDC power transfer

EVSE phase imbalance at the AC input connections are quantified from the quasi-steady-state testing at nominal conditions. As shown in Table 9, the average phase-to-phase current imbalance is 1.3%, while the maximum measured current phase-to-phase imbalance measured during all nominal condition steady-state testing is 3.8%.

Table 9. Phase-to-phase current imbalance during all steady-state power transfer tests.

	Max. Imbalance	Average Imbalance
EVSE2_1	3.8%	1.3%

Under nominal test conditions after the four-hour soak prior to testing, the standby power consumption is measured. Table 10 details the real and reactive power of EVSE2 in a standby state, not connected to a vehicle. Additionally, the standby power consumption is measured following several charge sessions. The standby power consumption of EVSE2 approximately 10 seconds after the completion of a charge session is the same power consumption as the standby power consumption before the start of the charge session.

Table 10. Standby power consumption (no power transfer).

	Real Power (W)	Reactive Power (VAR)
EVSE2	165	280

3.2 High-Utilization Test Results

EVSE characterization during high-utilization or repetitive power transfer sessions is conducted to determine the EVSE performance characteristics and the power consumption of the EVSE auxiliary control systems, including the CCS liquid-cooled cable thermal management system. Three full-power, 10-minute charge sessions are conducted consecutively with a small rest period between the charge sessions, as detailed in Table 5. In between each charge session, the charge cable is unplugged from the EV emulator and returned to the cable holster on the EVSE charge dispenser. This test sequence is representative of three EVs charging consecutively at one EVSE, with little time between the charge sessions.

The high-utilization testing of EVSE2_1, as shown in Figure 12, d the performance of the EVSE during the test sequence. The first charge session operated at full-power output (346 kW DC) for approximately six minutes, and then reduced to 90 AMP DC power transfer. During this charge session, the liquid-cooled CCS cable reaches a maximum temperature threshold that results in a current-limited state that only allows a 90 AMP DC power transfer maximum. The subsequent charge sessions are also limited to 90 AMP DC until the error state is cleared by cycling the main AC input power to the EVSE (i.e., hard reset).

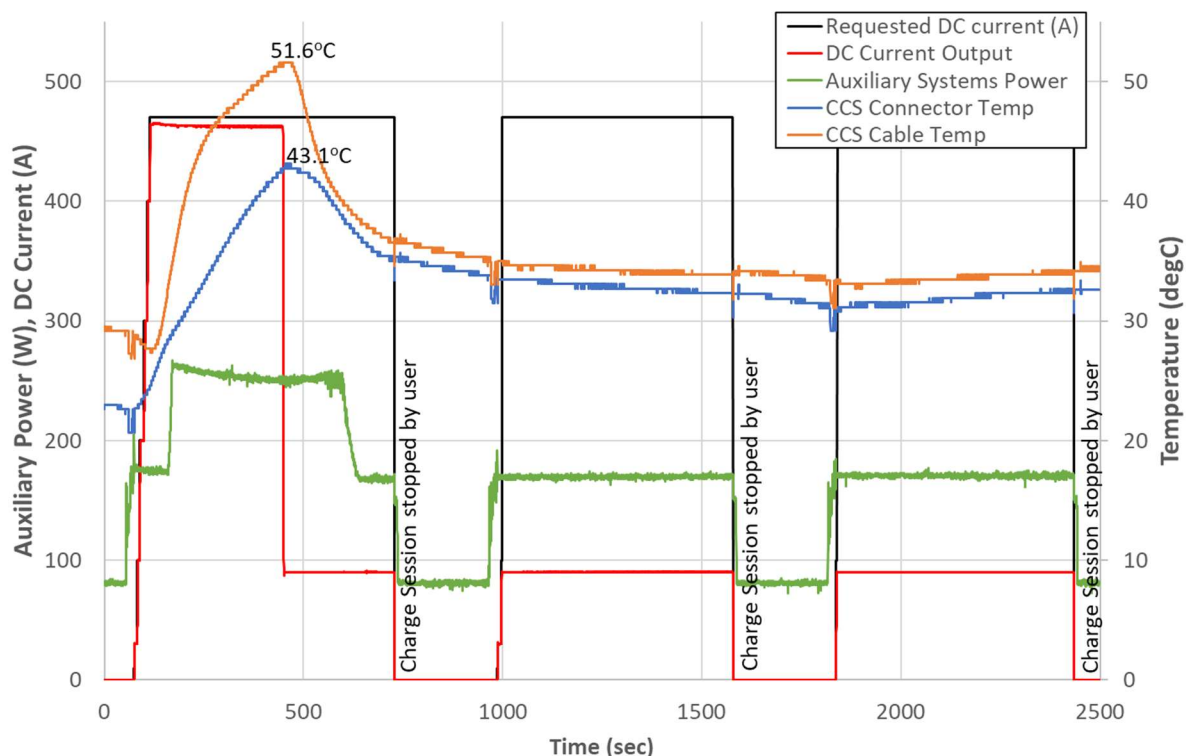


Figure 12. EVSE2_1 high-utilization test results at 750 VDC power transfer.

3.3 Off-Nominal Test Conditions Results

Voltage deviation, frequency deviation, and harmonics injection are characterized for EVSE2_1. The testing is conducted at Table 3 power transfer levels. Overall, for the off-nominal AC grid input test cases, the EVSE power transfer continues as requested, except when AC input voltage drops below 418 VAC (13% voltage sag), which results in the interruption of the power transfer from the EVSE to the EV, until the AC input voltage recovers to greater than 418 VAC. Additionally, the DC output current ripple is very low during the various test cases, except for the highest power transfer test conditions, as indicated by the high DC current ripple and large AC phase-to-phase current unbalance during the 350 kW power transfer and the 5% AC harmonics test condition. More details are provided in the following sections for each of the off-nominal test cases.

3.3.1 AC Voltage Deviation

Off-nominal grid conditions characterization is conducted for AC input voltage deviations following the procedures detailed in Table 6. The AC input voltage deviation included swell to 518 VAC and sag to 426 VAC. For all AC voltage deviation test conditions, the DC current is very

stable, the DC current ripple is very low, and the power transfer continues uninterrupted, as detailed in Table 11.

Table 11. Impact of AC input voltage deviation on DC output current.

Input AC Voltage Deviation Tests	Maximum DC Output Current	Minimum DC Output Current	Maximum DC output Current Ripple %
350 kW at 850 VDC	410.3 AMP	410.2 AMP	0.65%
150 AMP at 850 VDC	150.1 AMP	149.6 AMP	0.65%
500 AMP at 400 VDC	500.0 AMP	499.5 AMP	0.11%
150 AMP at 400 VDC	149.7 AMP	149.8 AMP	0.28%

3.3.2 AC Frequency Deviation

Off-nominal grid conditions characterization is conducted for AC input frequency deviations following the procedures detailed in Table 7. The AC input frequency is varied between 61.2 Hz and 58.8 Hz. During all the AC frequency deviation test conditions, the DC current is stable, the DC current ripple is low, and the power transfer continues uninterrupted, as detailed in Table 12.

Table 12. Impact of AC frequency deviation on DC output current.

Input AC Frequency Deviation Tests	Maximum DC Output Current	Minimum DC Output Current	Maximum DC output Current Ripple %
350 kW at 850 VDC	410.3 AMP	410.8 AMP	0.75%
150 AMP at 850 VDC	149.8 AMP	149.8 AMP	0.75%
500 AMP at 400 VDC	499.7 AMP	499.7 AMP	0.17%
150 AMP at 400 VDC	149.8 AMP	149.7 AMP	0.43%

3.3.3 AC Harmonics Injection

Off-nominal grid conditions characterization is conducted for 5% AC input harmonics injection during power transfer test conditions following the procedures detailed in Table 8. During the 5% harmonics injection testing, a distorted AC waveform is input to the EVSE. The DC current stays stable and closely follows the requested current, except for the highest power transfer test case (350 kW at 850 VDC) in which the DC current varies by more than 4 AMP DC. During the 400 V DC test cases, the DC current ripple is very low. However, during the 850 V DC test cases, the DC current ripple exceeds 14% for the 350 kW test case. Additionally, during the 350 kW test case at 850 VDC, the phase-to-phase AC current unbalance exceeded 18.9% during 5% AC harmonics injection. These results are detailed in Table 13. Once the 5% harmonics injection ceased, the phase-to-phase AC current unbalance returned to <1.9% unbalance.

Table 13. Impact of 5% AC voltage harmonics on DC output current.

Input AC Harmonics Injection Tests	Maximum DC Output Current	Minimum DC Output Current	Maximum DC Output Current Ripple %
350 kW at 850 VDC	405.3 AMP	409.7 AMP	14.2%
150 AMP at 850 VDC	149.8 AMP	149.8 AMP	4.32%

500 AMP at 400 VDC	500.0 AMP	499.9 AMP	0.48%
150 AMP at 400 VDC	149.8 AMP	149.7 AMP	0.49%

3.4 OCPP Smart Energy Management Test Results

Latency and ramp rate response of the EVSE power transfer is characterized after a smart energy management curtailment request executed via Open Charge Point Protocol (OCPP) is issued. The OCPP version used during the EVSE2_1 characterization is OCPP 1.6J. This characterization is conducted at two power transfer conditions: 500 AMP at 400 V DC and 350 kW at 850 V DC. For each power transfer condition, three types of curtailment requests are conducted, each at 65 AMP and 54 kW. The three curtailment request types are *ChargePointMaxProfile*, *TxDefaultProfile*, and *TxProfile*.

The curtailment requests are not scheduled events. Instead, to ensure accurate latency measurement without the need for synchronized clocks across all test systems, each manually initiated request message is measured by the same data acquisition system that records all the other testing measurements. This enables high accuracy in quantifying the latency from the curtailment request to the electrical response of the EVSE.

All the curtailment requests successfully result in power transfer reduction soon after the request is initiated, and the power transfer resumes at the previously requested level soon after the curtailment request is cleared. The *ClearChargingProfile* request message is used to end the curtailment.

The latency of EVSE2_1 power transfer to respond to the curtailment request is roughly 3 seconds on average and varies greatly ranging from 0.6 seconds to 5.7 seconds under ideal laboratory conditions. Table 14 details the results for the latency of the curtailment requests during the tested power transfer initial conditions. Table 15 details the results when the curtailment request ends, resulting in the power transfer ramping up to the previously requested steady-state power transfer test condition.

Table 14. Curtailment latency and ramp rates for OCPP curtailment requests.

	Average Latency (s)	Minimum Latency (s)	Maximum Latency (s)	Average Ramp Rate (AMP/s)
350 kW at 850 V operation	3.5	0.6	4.7	-200.6
500 AMP at 400 V operation	2.7	1.1	5.2	-64.1

Table 15. Curtailment latency and ramp rates for OCPP clear curtailment requests.

	Average Latency (s)	Minimum Latency (s)	Maximum Latency (s)	Average Ramp Rate (AMP/s)
350 kW at 850 V operation	3.4	1.0	5.7	171.7
500 AMP at 400 V operation	3.6	1.3	5.7	44.8

For the range of test cases and test conditions, the ramp rates vary considerably from -200 AMP/s to -64 AMP/s. For each initial power transfer condition (e.g., 350 kW at 850 VDC), the ramp rates are mostly consistent; however, there is significant variation in ramp rates across the differing power transfer initial conditions. This does not appear to correlate to a constant ramp duration that is proportional to the initial power transfer (e.g., longer duration for high-power initial condition). The 350 kW at 850 VDC power transfer initial condition curtailment ramp duration is approximately 2.0 seconds, whereas the 500 AMP at 400 VDC (200 kW) power transfer test condition ramp duration is approximately 3.2 seconds. Additional lower power initial conditions result in ramp durations of 0.6 and 1.1 seconds for 60 kW and 125 kW, respectively.

Figure 12 and Figure 13 show the power transfer ramp down characteristics resulting from OCPP curtailment requests. Note that each curtailment request is initiated at time indicated by the Y-axis intersection (time = 60 seconds for Figure 13 and time = 30 seconds for Figure 14).

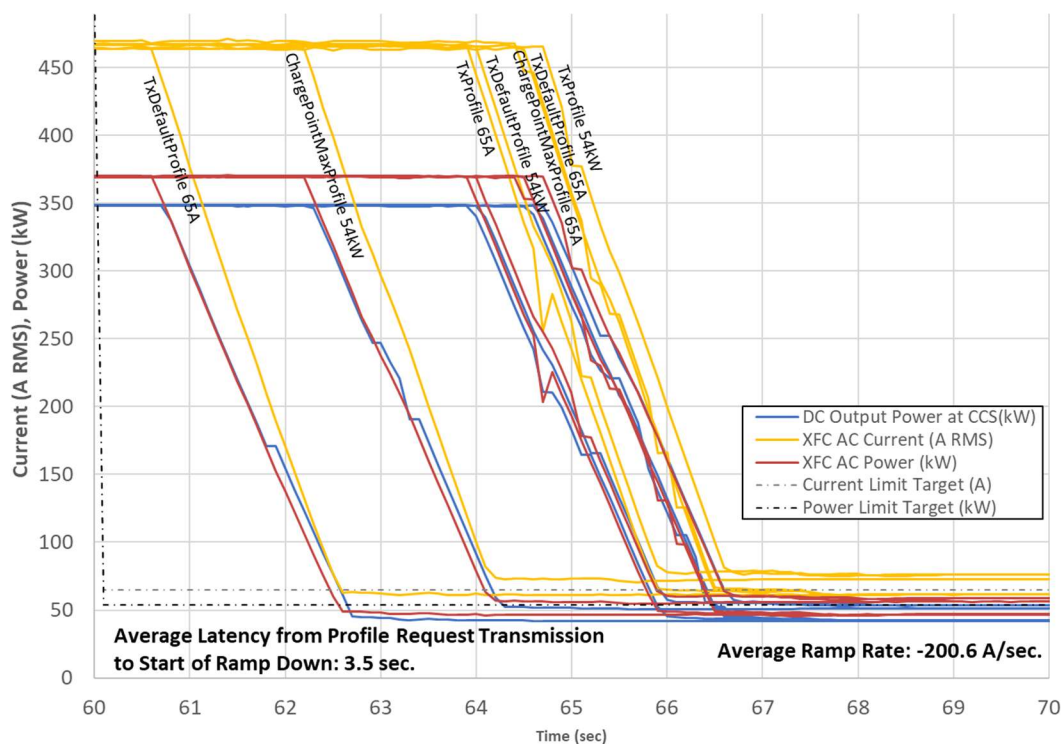


Figure 13. Response to OCPP curtailment request during 350 kW at 850 VDC power transfer.

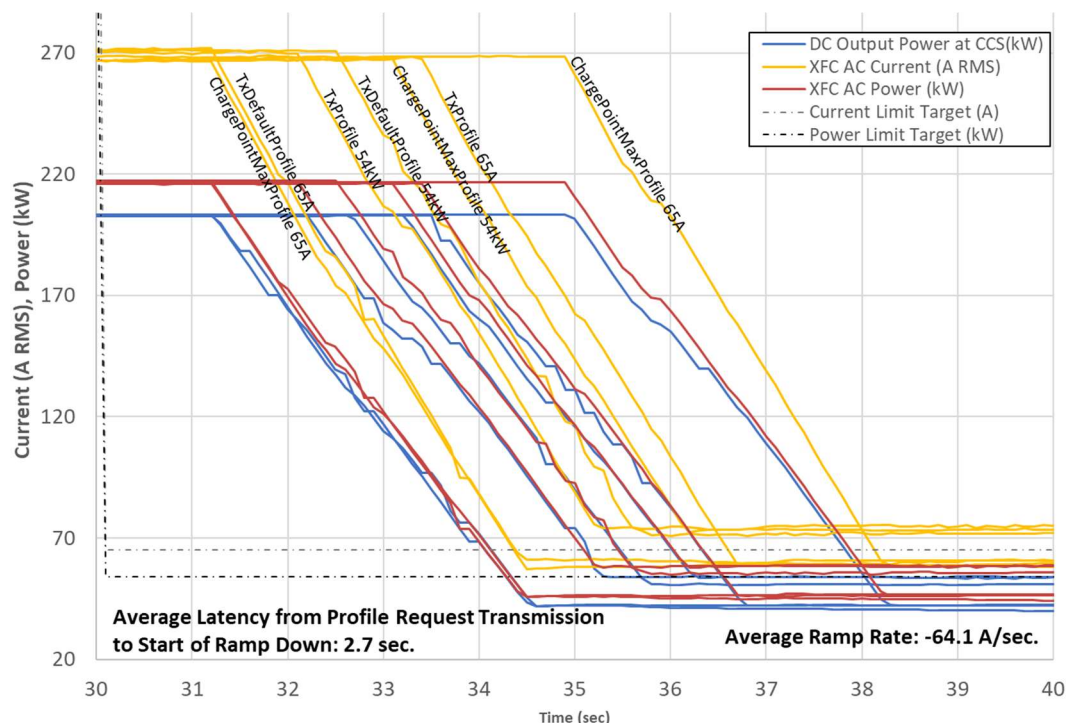


Figure 14. Response to OCPP curtailment request during 500 AMP at 400 VDC power transfer.

For the range of conditions and test cases, the ramp up rates after a curtailment event is cleared varies considerably, from 172 AMP/s to 45 AMP/s, as shown in Figure 15 and Figure 16. Note the curtailment request is initiated at the time indicated by the Y-axis intersection (time = 60 seconds for Figure 15 and time = 30 seconds for Figure 16). Again, as seen with curtailment ramp down rates, the ramp up rates after a curtailment event are consistent for the initial power transfer condition but vary greatly across differing initial power transfer conditions.

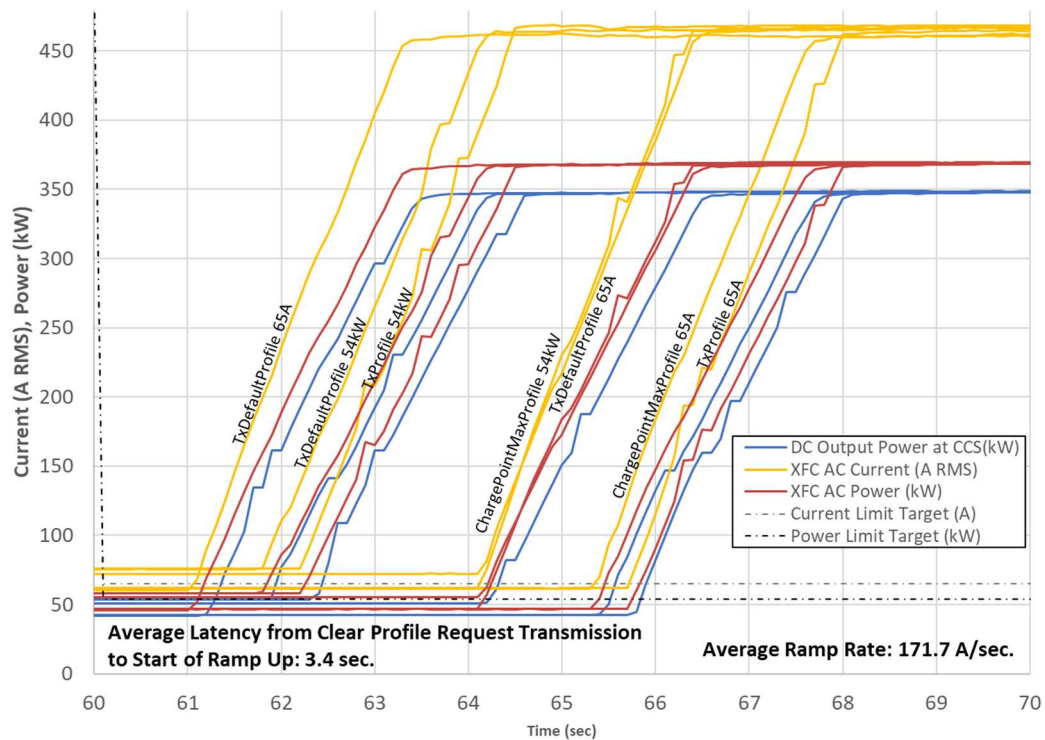


Figure 15. Response to OCPP clear curtailment request during 350 kW at 850 VDC power transfer.

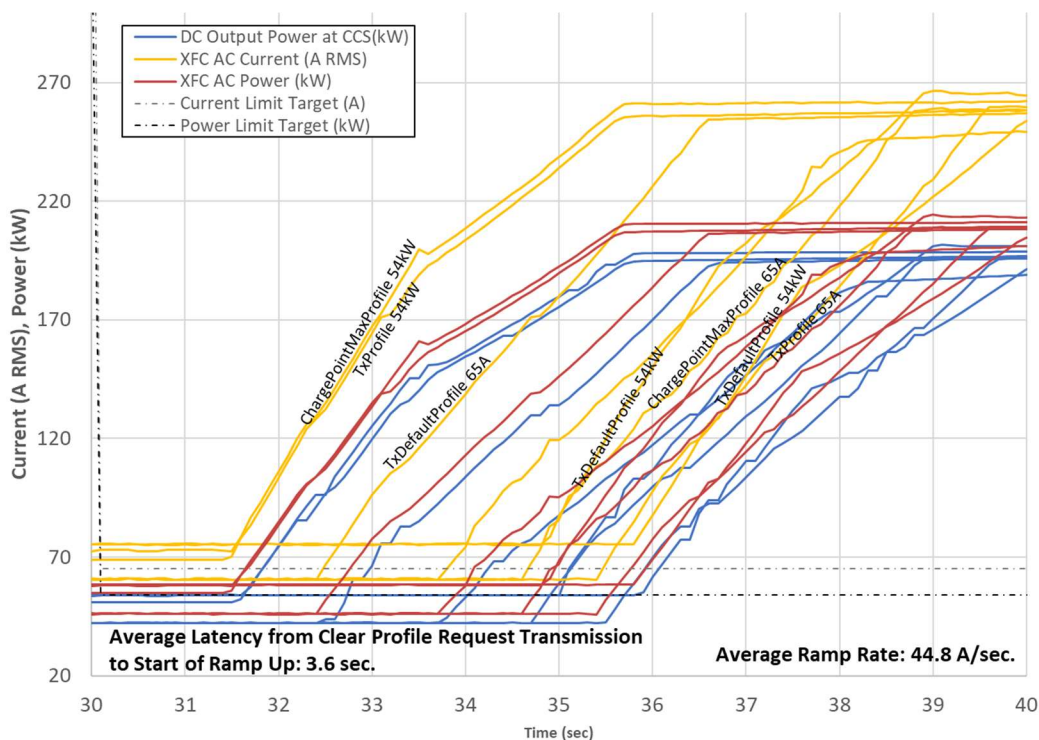


Figure 16. Response to OCPP clear curtailment request during 500 AMP at 400 VDC power transfer.

Per OCPP1.6 specifications, current curtailment requests are specified for AC input current. Power curtailment requests may be specified for either AC input power or DC output power transfer, as implemented by the EVSE manufacturer. For the EVSE curtailment response and latency characterization, the specific requests and results are listed in Table 16 and Table 17.

The EVSE2_1 DC power transfer, total AC power consumption, and total AC input current during each curtailment request are measured. These measurements enable a direct comparison between the curtailment requested value and the EVSE2_1 performance during the curtailment event. This measured power or AC input current during the requested curtailment varied slightly across the numerous test cases. Most test cases resulted in the power or current slightly below the curtailment request value; however, a few test cases resulted in up to 2.2% higher power transfer than the curtailment request, as shown in Table 16 and Table 17.

Table 16. Steady-state power transfer characteristics during OCPP curtailments.

Curtailment Request during 350 kW at 850 VDC Operation	Curtailment Request	Steady State Measured Current or Power Transfer	Percent Difference from Request
ChargePointMaxProfile 65 AMP	65.0 AMP	61.1 AMP	-6.0%
ChargePointMaxProfile 54 kW	54.0 kW AC	55.2 kW AC	+2.2%
TxDefaultProfile 65 AMP	65.0 AMP	60.4 AMP	-7.1%
TxDefaultProfile 54 kW	54.0 kW DC	54.3 kW DC	+0.6%
TxProfile 65 AMP	65.0 AMP	62.1 AMP	-4.5%
TxProfile 54 kW	54.0 kW DC	54.3 kW DC	+0.6%

Table 17. Steady-state power transfer characteristics during OCPP curtailments.

Curtailment Request during 500 AMP at 400 VDC Operation	Curtailment Request	Steady State Measured Current or Power Transfer	Percent Difference from Request
<i>ChargePointMaxProfile</i> 65 AMP	65.0 AMP	60.8 AMP	-6.5%
<i>ChargePointMaxProfile</i> 54 kW	54.0 kW AC	55.0 kW AC	+1.9%
<i>TxDefaultProfile</i> 65 AMP	65.0 AMP	60.5 AMP	-6.9%
<i>TxDefaultProfile</i> 54 kW	54.0 kW DC	53.9 kW DC	-0.2%
<i>TxProfile</i> 65 AMP	65.0 AMP	60.4 AMP	-7.1%
<i>TxProfile</i> 54 kW	54.0 kW DC	54.0 kW DC	0.0%

3.5 Summary of Conductive EVSE Characterization Results and Analysis

EVSE characterization results have been provided for a 350-kW conductive EVSE across a wide range of operation conditions. These results are intended to support industry stakeholders, decision makers, modeling and simulation efforts, and many other groups developing and deploying advanced electrified transportation systems. The results include steady-state performance characteristics under nominal conditions, off-nominal grid input performance, high-utilization power transfer characteristics, and transient performance during energy management curtailment requests.

4 Wireless Power Transfer EVSE Characterization Results and Analysis

4.1 Nominal Operating Conditions Test Results

4.1.1 Efficiency Characterization Results

At nominal operating conditions in alignment and at nominal airgap, the efficiency characteristics of the system for three different resistive load conditions, as a function of the output power with 10-kW power increments, are provided in Figure 17. According to this Figure 17, for up to 30 kW output power, system efficiency increases from about 93% to 94.1%, and it stays above 94% within 30–100% loading condition.

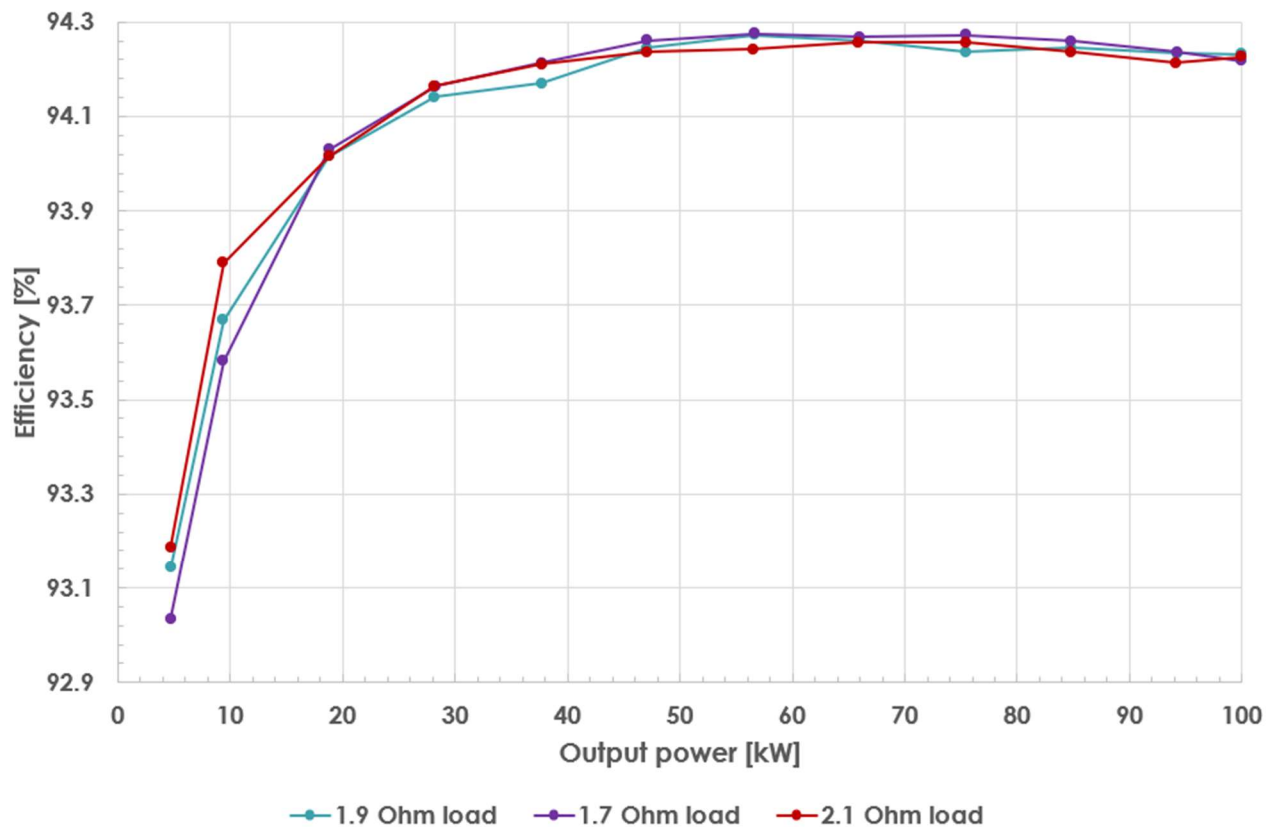


Figure 17. Efficiency characteristics of the system at nominal conditions for three different resistive load conditions as a function of output power.

As an example, the power analyzer screenshot at the nominal power (100-kW output) is shown in Figure 18 for the 1.9 Ohm load resistance condition.

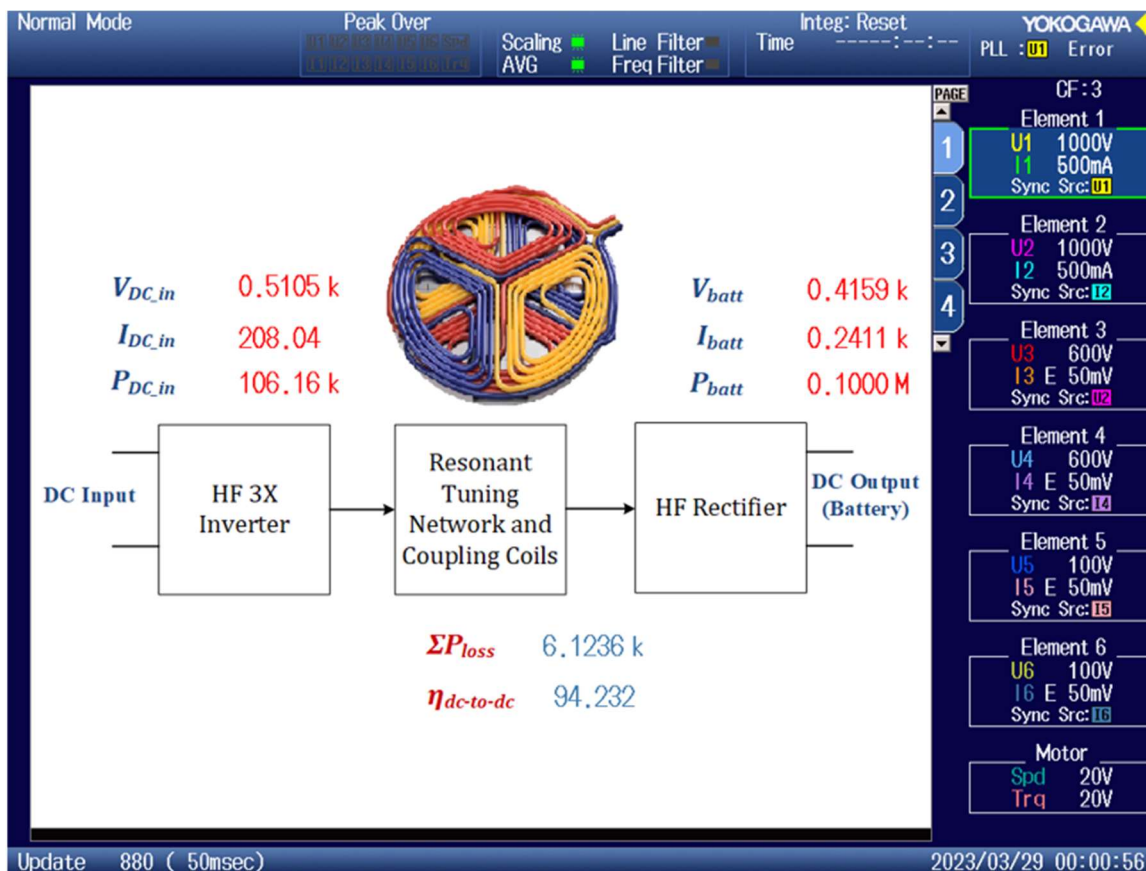


Figure 18. Power analyzer screenshot for 1.9 Ohm load resistance at 100 kW nominal output power condition.

Efficiency characterization of EVSE7 is given in Figure 19 under different power levels with 10-kW increments for four different battery voltage levels. As shown in this figure, while the light load efficiency is relatively lower, above 30 kW power transfer level, efficiency is almost constant. Figure 20 shows the efficiency snapshot at 390 V battery voltage condition with 100 kW power transfer that results in about 94.44% efficiency. Note that the battery voltage rises to about 403 V with 248 AMP battery charge current due to the battery's internal resistance, which is about 5 mΩ.

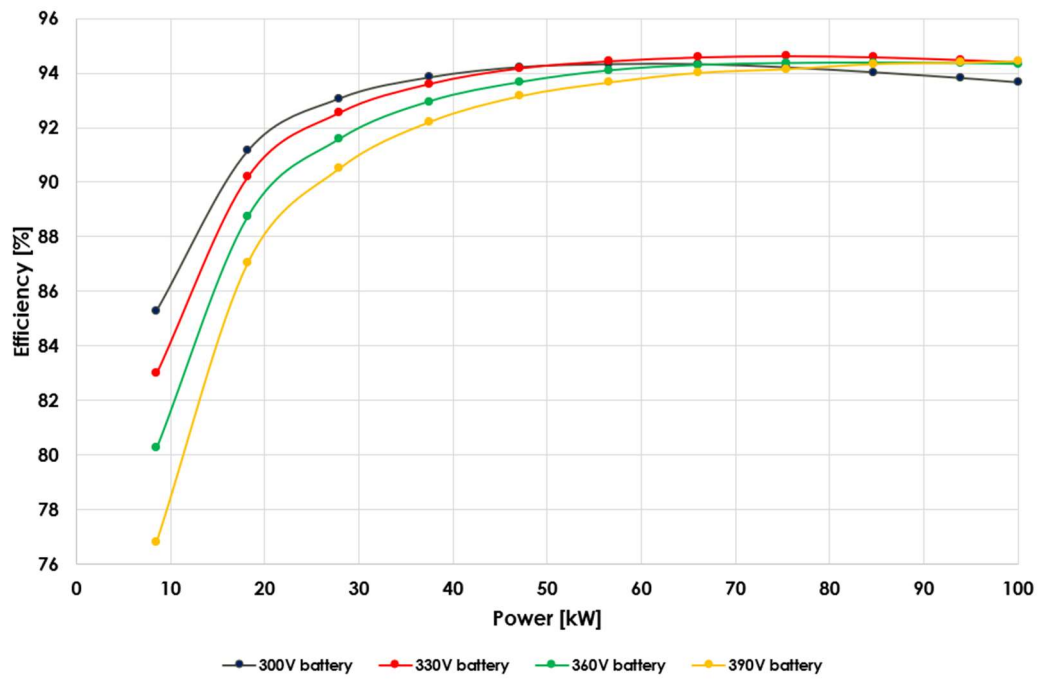


Figure 19. Efficiency characterization of EVSE7 at four battery voltages at different power levels.

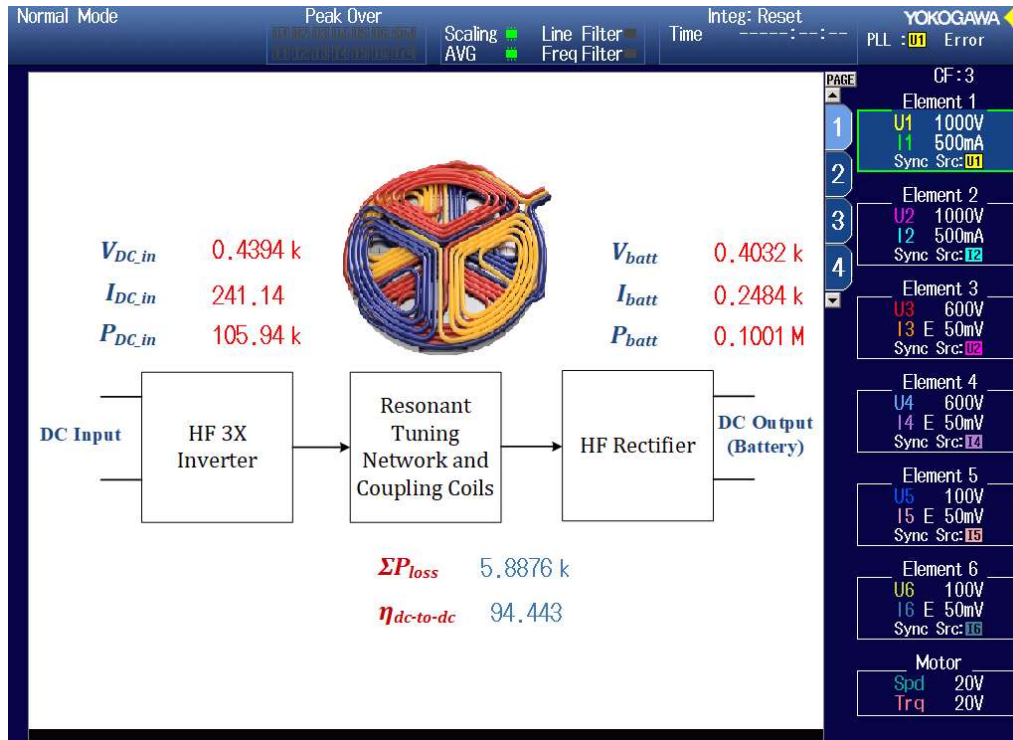


Figure 20. System efficiency (94.44%) with 390 V battery voltage with 100 kW load power.

4.1.2 Electromagnetic Field and Electric Field Emissions

Under the nominal conditions (fully aligned with a nominal airgap of 5 inches), the EM-field emissions are measured at distances of 0.8 m, 0.9 m, and 1 m from the center of the secondary coil at 100 kW nominal power transfer conditions. The magnetic field emissions are measured with a NARDA EHP-200 isotropic field sensor and are illustrated shown in Figure 21. Similarly, electric field emissions are also measured at distances of 0.8 m, 0.9 m, and 1 m from the center of the secondary coil at 100 kW nominal power transfer conditions, and the measurement results are presented in Figure 22.

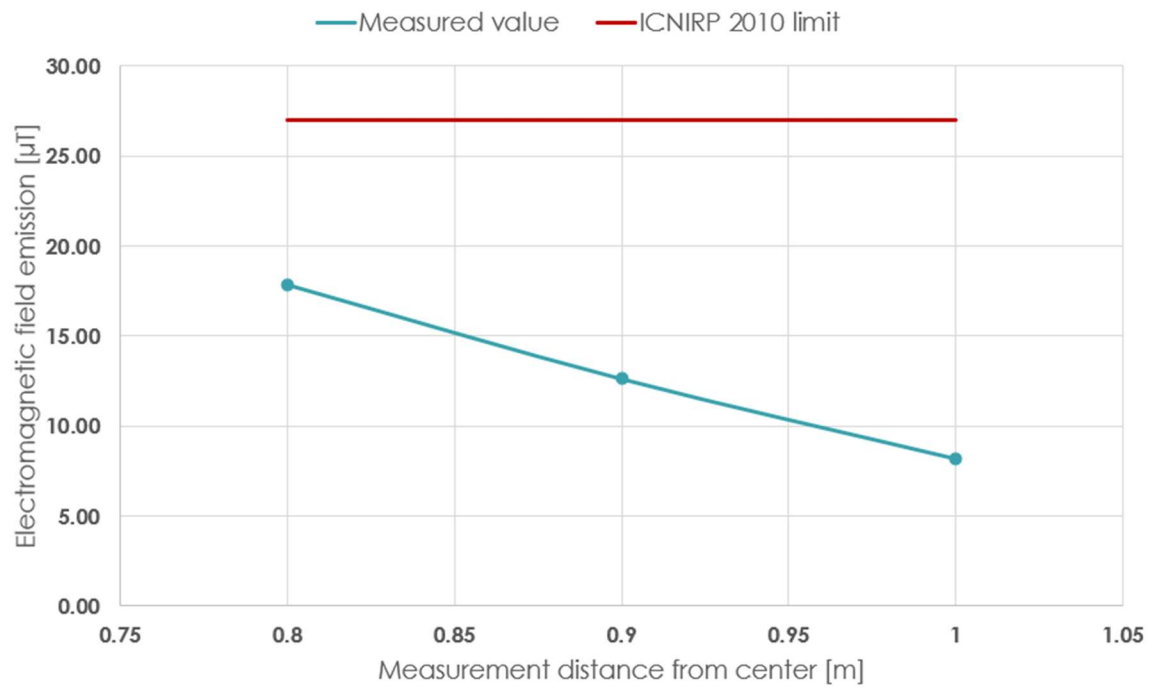


Figure 21. Electromagnetic field emissions as a function of distance from the center of the secondary coupler with 100 kW power transfer condition.

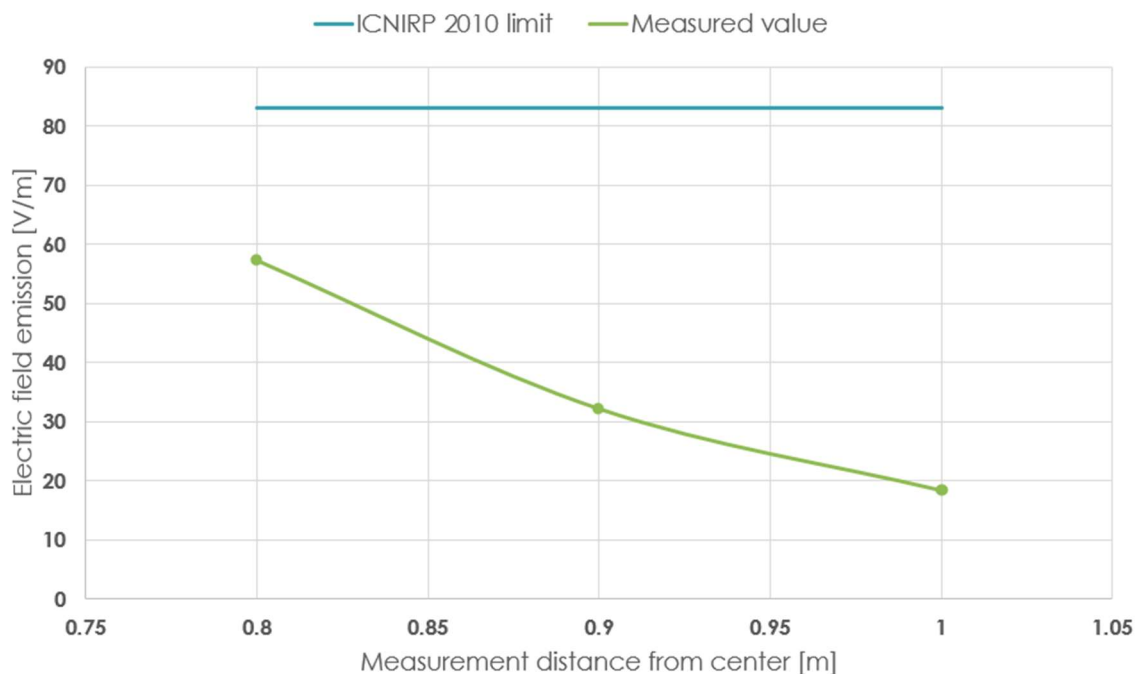


Figure 22. Electric field emissions as a function of distance from the center of the secondary coupler with 100 kW power transfer condition.

4.2 Off-Nominal Operating Conditions Test Results

For the off-nominal test conditions, the receiver coil was displaced or moved into a certain position to create the misalignment for x and y, or in x and y combined directions, to evaluate the system performance under these conditions. In addition, off-nominal conditions include angular misalignments in yaw, roll, and pitch angles ($\Delta\Phi$, $\Delta\phi$, $\Delta\theta$, respectively). The definition of these off-nominal conditions is illustrated in Figure 23, where the x misalignment is toward the direction of travel (longitudinal), y misalignment is lateral, yaw angle indicates angular misalignment, roll angle indicates lateral angular misalignment, and pitch angle indicates longitudinal angular misalignment. In Figure 24, the relative receiver coil position is provided for a worst-case misalignment condition as an example.

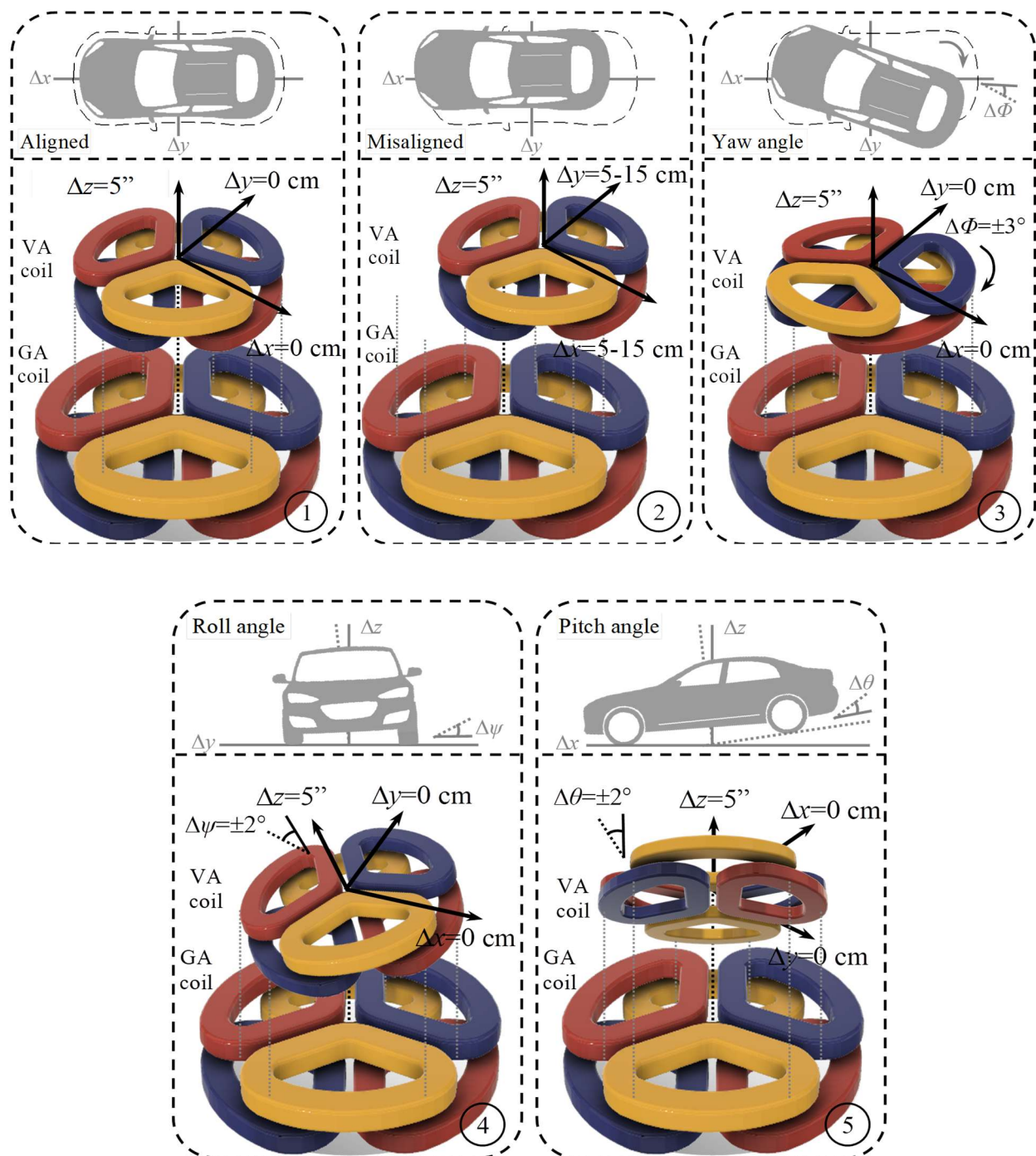


Figure 23. Off-nominal condition definitions with respect to coil positions.

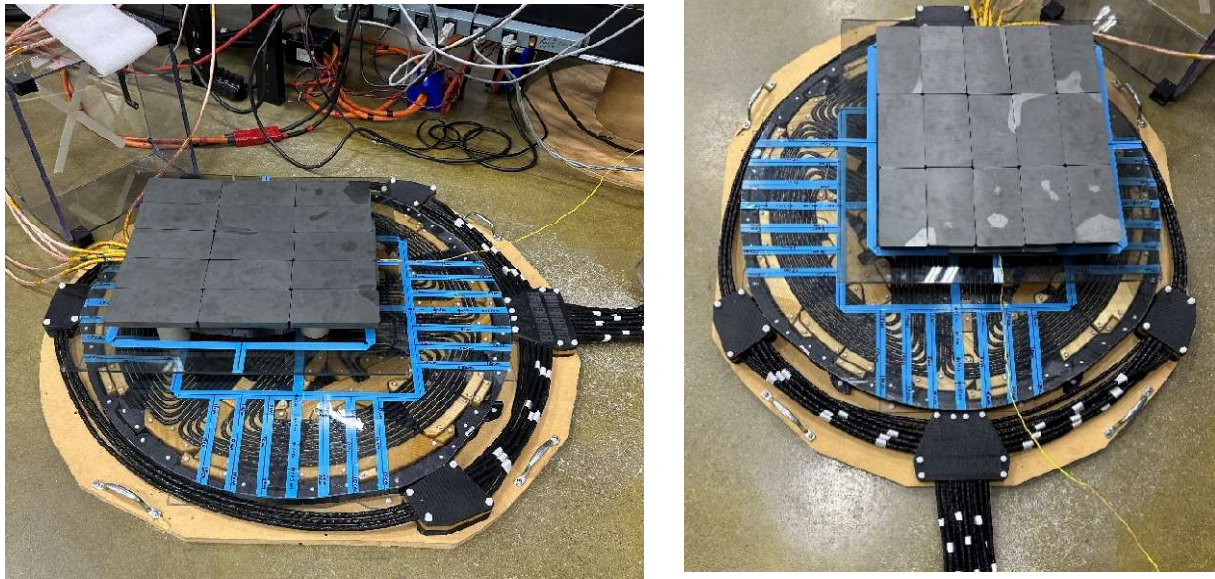


Figure 24. $\Delta x=7.5\text{cm}$ and $\Delta y=10\text{cm}$ misalignment position from two different view angles.

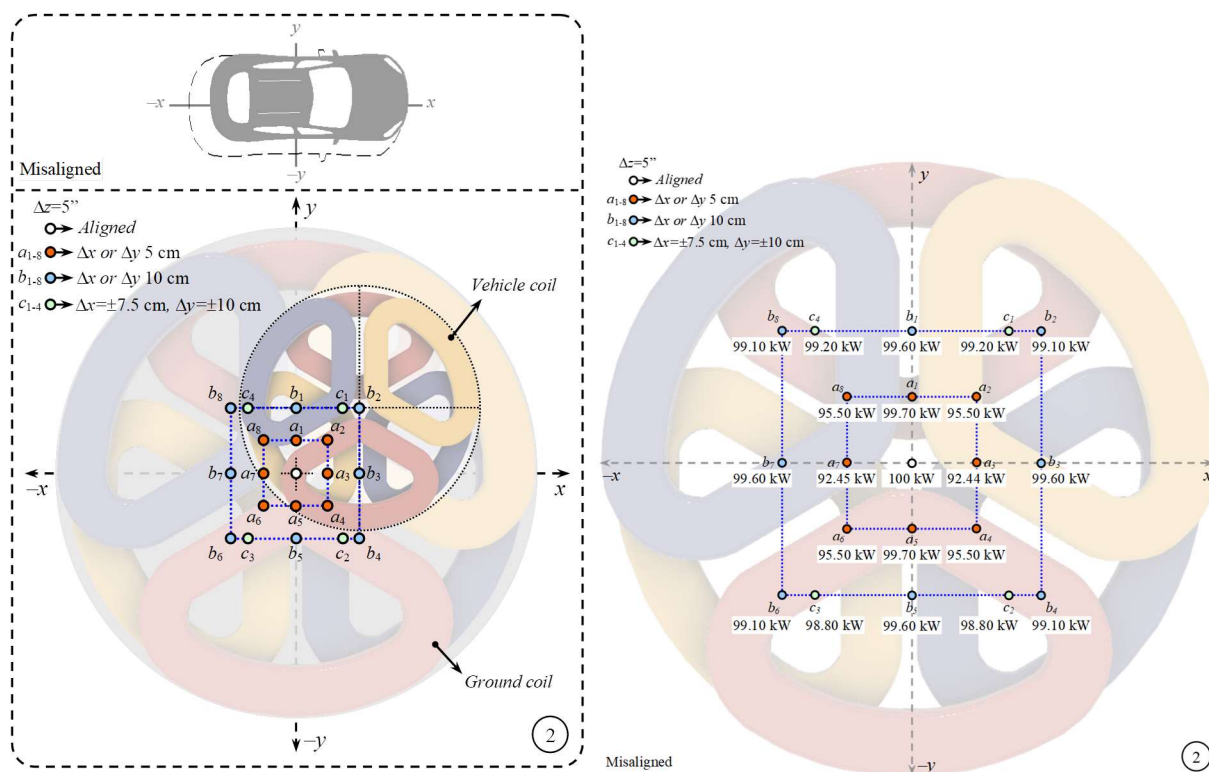


Figure 25. Illustration of misaligned positions, including Δx and Δy misaligned positions and the power levels, achieved for each condition.

Power transfer levels achieved for the full set of misaligned positions are shown in Figure 25. The WPT system can maintain the same power transfer for most of the a, b, and c positions that have certain degrees of misaligned positions. The only slight power reduction occurred in positions a1 to a8. The mutual inductance imbalance caused by the misalignment changes the effective loading at the inverter output, and some of the phases move to the edge of shifting to capacitive operation, losing the zero-voltage-switching condition. This move results in increased stress and turn-on voltage overshoots at the inverter output voltages. While the silicon carbide power modules are rated for 1200 V, and these voltage overshoots were limited to 250 V over the operating voltage, the team did not take any risks to increase the power transfer to the full-power rating of 100 kW under these conditions. Most likely, the power modules would easily handle these voltage overshoot conditions without any damage to the hardware.

The full efficiency characteristics under misaligned conditions are mapped and illustrated in a 3-dimensional graph in Figure 26.

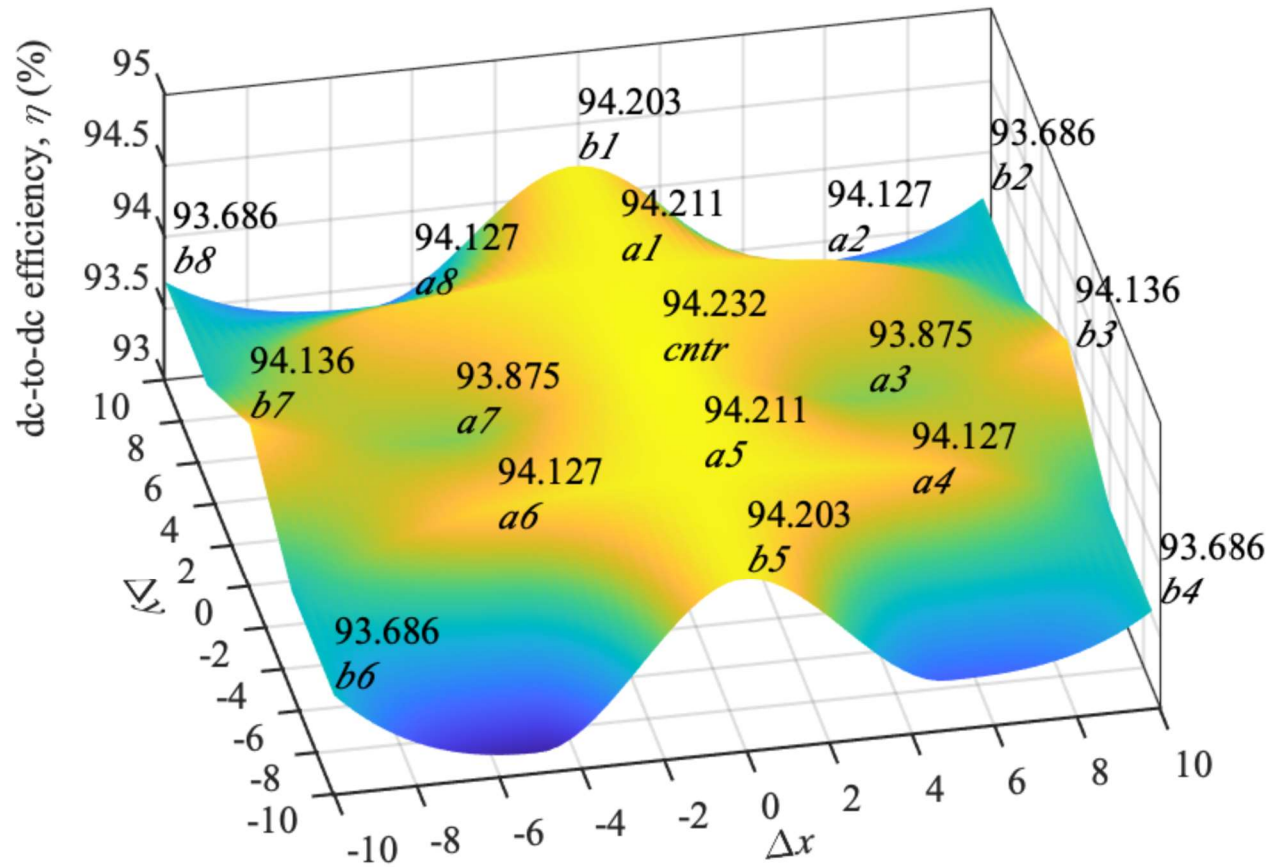


Figure 26. Efficiency map of the system under misaligned conditions.

The efficiency characteristics are represented with contour lines in Figure 27, as shown below. According to Figure 26 and Figure 27, the power transfer can be maintained under all misaligned conditions with almost the same efficiency as when the maximum efficiency reduction is $<0.6\%$ even in worst cases.

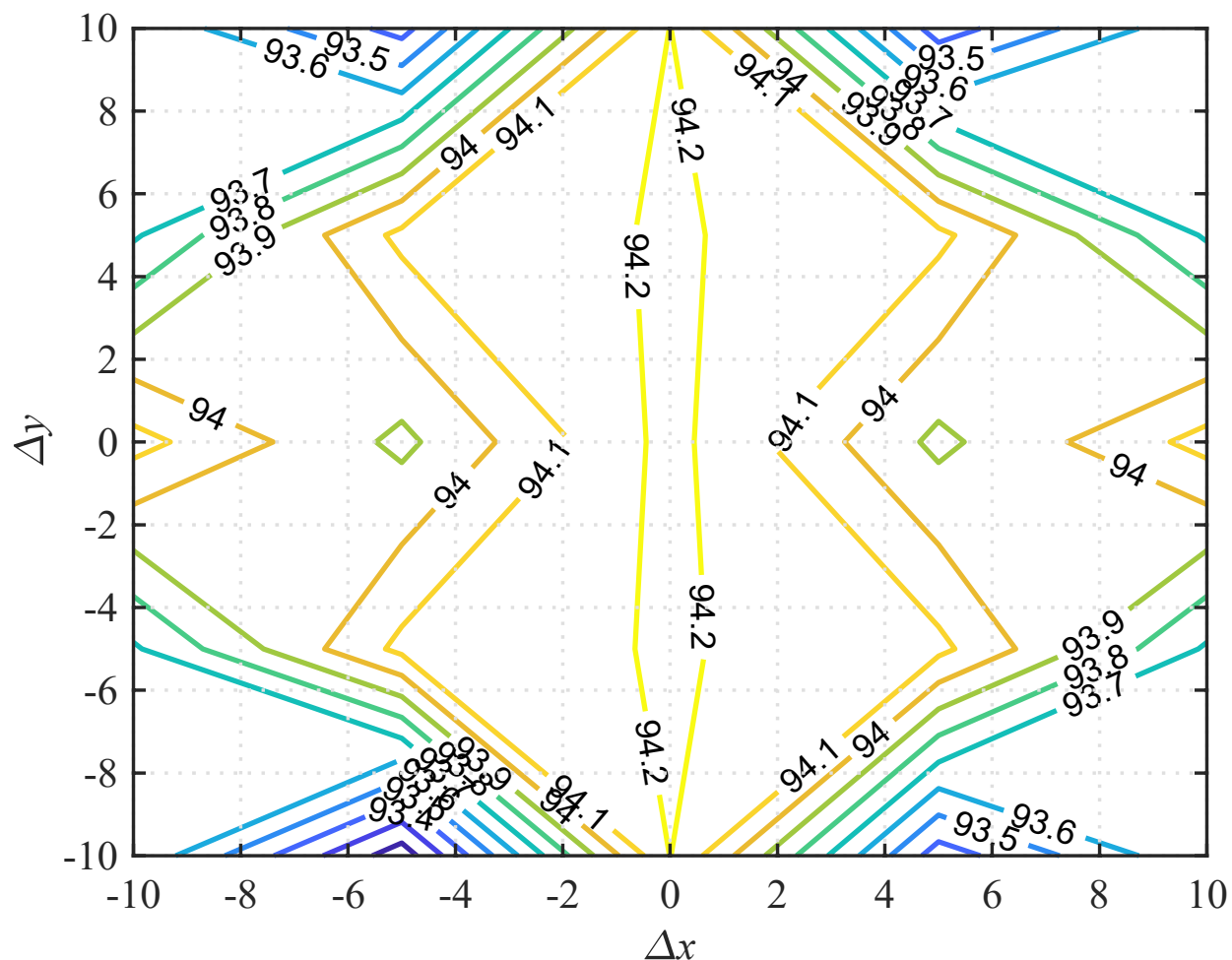


Figure 27. Efficiency map of the system under misaligned conditions in contour lines.

System performance under all off-nominal conditions, including the x, y, x-y misalignments, and angular misalignments, including yaw, roll, and pitch, are summarized in Table 18. Results include the data for the nominal conditions, including resistive load and battery load conditions, and the data for the off-nominal conditions, including the misalignments at the selected a2, b2, and c1 point positions as well as the yaw, roll, and pitch angular misalignments. Results include the input voltage, current, power, the inverter output phase-a voltage, current, power, the rectifier input voltage, current, power, and the load voltage, current, and power along with the efficiency numbers for each of these conditions. As shown in Table 18, efficiency is usually above 94%, with one exception with similar power transfer achieved for all nominal and off-nominal conditions.

Table 18. System performance under all nominal and off-nominal conditions.

Charging Positions		DC Input V_{dc_in} , i_{dc_in} , P_{dc_in}	Primary Side V_{Ag} , i_{Ag} , P_{Ag}	Secondary Side V_{Xv} , i_{Xv} , P_{Xv}	DC Output V_{bat} , i_{bat} , P_{bat}	η (%)
1: Aligned (resistive load @1.9 Ω) $\Delta z = 5''$		510.50 V	513.43 V	412.00 V	415.90 V	94.232
		208.04 AMP	72.587 AMP	69.570 AMP	241.10 AMP	
		106.16 kW	37.286 kW	28.662 kW	100.00 kW	
2: Aligned (Battery load @390V) $\Delta z = 5''$		439.4 V	435.7 V	403.58 V	403.2 V	94.443
		241.14 AMP	103.19 AMP	103.39 AMP	248.4 AMP	
		105.94 kW	37.74 kW	35.40 kW	100.1 kW	
3: Misaligned	a ₂ point $\Delta x = 5\text{cm}$ $\Delta y = 5\text{cm}$	452.00 V	457.42 V	416.40 V	416.50 V	94.127
		234.02 AMP	81.170 AMP	82.340 AMP	239.40 AMP	
		105.76 kW	44.434 kW	34.286 kW	99.500 kW	
	b ₂ point $\Delta x = 10\text{cm}$ $\Delta y = 10\text{cm}$	532.30 V	537.28 V	415.40 V	415.5 V	93.686
		198.88 AMP	70.882 AMP	87.090 AMP	239.60 AMP	
		105.76 kW	38.083 kW	36.177 kW	99.100 kW	
	c ₁ point $\Delta x = 7.5\text{cm}$ $\Delta y = 10\text{cm}$	534.40 V	542.22 V	418.00 V	415.70 V	93.767
		198.09 AMP	70.199 AMP	70.090 AMP	239.40 AMP	
		105.79 kW	38.063 kW	29.297 kW	99.200 kW	
4: Yaw angle $\Delta\Phi = \pm 3^\circ$		425.00 V	430.27 V	416.50 V	416.20 V	94.576
		249.42 AMP	86.352 AMP	89.330 AMP	241.30 AMP	
		105.98 kW	37.154 kW	37.205 kW	100.20 kW	
5: Roll angle $\Delta\psi = \pm 2^\circ$		452.90 V	458.35 V	416.20 V	416.10 V	94.494
		234.16 AMP	82.667 AMP	89.090 AMP	241.30 AMP	
		106.01 kW	37.890 kW	37.079 kW	100.20 kW	
6: Pitch angle $\Delta\theta = \pm 2^\circ$		463.10 V	462.81 V	418.40 V	415.90 V	94.403
		229.01 AMP	79.124 AMP	78.430 A	241.10 AMP	
		106.02 kW	36.619 kW	32.815 kW	100.10 kW	

Since the yaw angle of $\Delta\phi = \pm 3^\circ$ was physically very insignificant, the system was also tested at $\Delta\phi = 15^\circ$, 30° , and 45° rotational yaw angle misalignments to exploit the characteristics at more extreme angular misaligned parking conditions. These yaw angle (rotational) misalignment conditions resulted in 94.58%, 94.61%, and 94.59% efficiencies, respectively. The slight increase in efficiency was likely due to the improved mutual inductance and improved balancing between phases under these rotational conditions since the nominal angular position has 180° between the wire exit routes of the transmitter and the receiver. As an example, the 30° yaw angle rotational misalignment efficiency snapshot under 100 kW power transfer condition is presented in Figure 28.

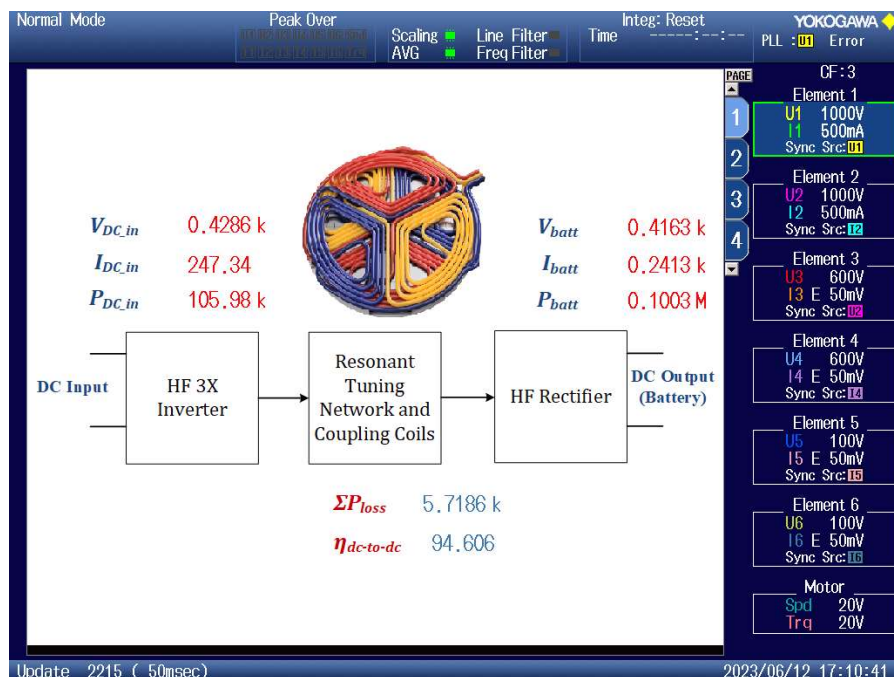


Figure 28. System efficiency at 100 kW power transfer with 30° yaw angle rotational misaligned condition.

The other off-nominal condition tested in this study includes increasing the airgap by about 2 inches and repeating the nominal 100 kW power transfer while the couplers are fully aligned. This resulted in the efficiency reducing to 93.49% at this peak power level, which is expected due to increased inverter output currents from reduced coupling factor. The coupling coils with 7 inches z-gap are shown in Figure 29, while the efficiency snapshot at 100 kW full-power transfer is shown in Figure 30.

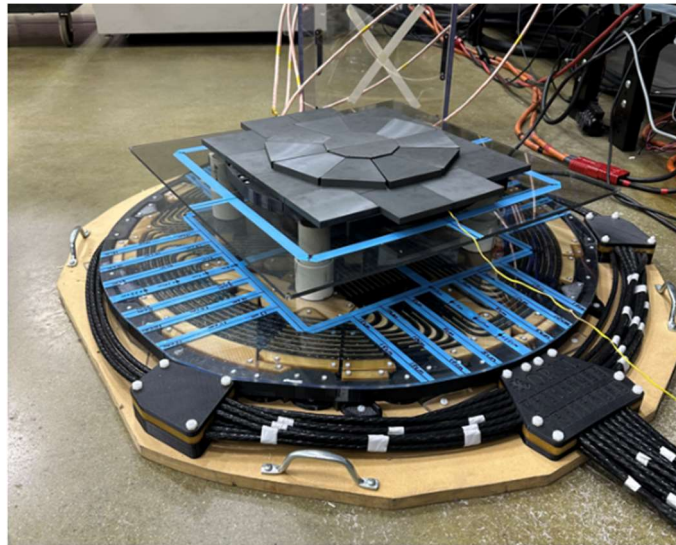


Figure 29. Coupling coils with increased airgap to 7 inches.

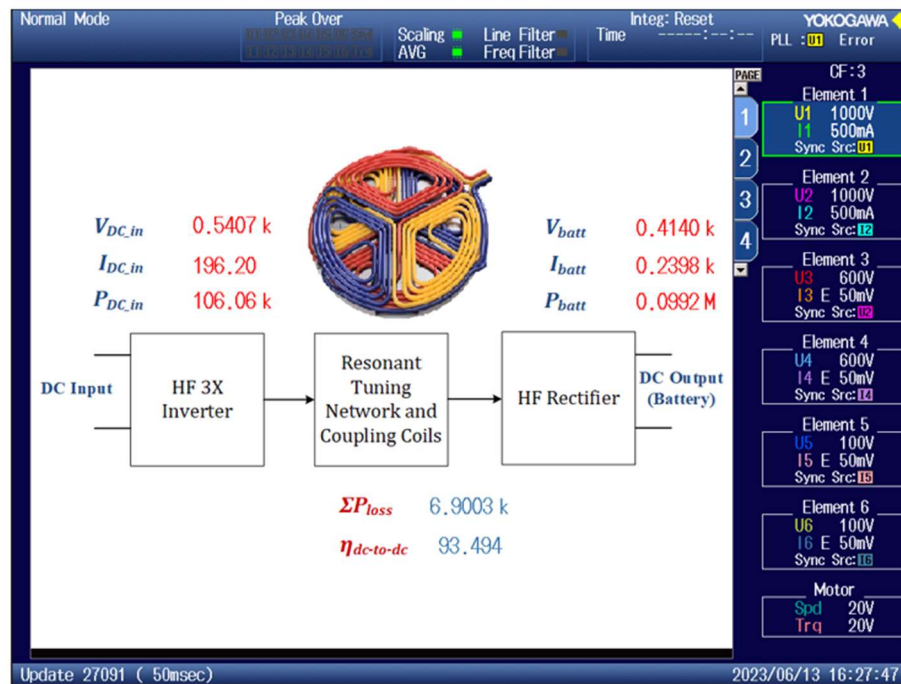


Figure 30. System efficiency at 100 kW power transfer with increased airgap condition.

